

# Cellular Automaton Growth on $\mathbb{Z}^2$ : *Theorems, Examples, and Problems*

JANKO GRAVNER  
Mathematics Department  
University of California  
Davis CA 95616  
gravner@feller.ucdavis.edu

DAVID GRIFFEATH  
Mathematics Department  
University of Wisconsin  
Madison WI 53706  
griffeat@math.wisc.edu

To appear in *Advances in Applied Mathematics*  
(Definitive version, April 1998)

**Abstract.** We survey the phenomenology of crystal growth and asymptotic shape for two-dimensional, two-state cellular automata. In the most tractable case of *Threshold Growth*, a detailed rigorous theory is available. Other less orderly examples with recursively computable updates illustrate the broad range of behavior obtained from even the simplest initial seeds and update rules. Still more exotic cases seem largely beyond the scope of exact analysis, but pose fascinating problems for experimentalists. The paper concludes with a discussion of connections between deterministic shape theory and important corresponding questions for systems with random dynamics.

1991 *Mathematics Subject Classification.* Primary 52A10.

*Key words and phrases.* Cellular automaton, crystal growth, shape theory.

*Running head :* CELLULAR AUTOMATON SHAPES

# Cellular Automaton Growth on $\mathbb{Z}^2$ : *Theorems, Examples, and Problems*

JANKO GRAVNER, DAVID GRIFFEATH

## 1. Introduction

In its simplest form, a *cellular automaton* (CA) is a sequence of configurations on a lattice which proceeds by iterative application of a local, homogeneous update rule. The ubiquitous example is Conway's Game of Life [BCG], [Gar2]. Cellular automata were originally proposed in the late 1940s by Ulam [Ula] and von Neumann [vN] as prototypes for complex interacting systems capable of self-reproduction. Since that time the CA paradigm has been used to model spatial dynamics across the spectrum of applied science, and a vast literature, overwhelmingly empirical, has developed. Seminal papers in the area include [FHP], [Hol], [JM], and [WR]. For some more recent exemplary applications to physics, chemistry and biology, see [AL], [LDKB], [NM], and the review article [EE-K]. Now, as parallel architectures become increasingly prevalent in computer design, modelers continue to be drawn to CA systems and their extensions to inhomogeneous environments and evolutionary dynamics.

During the past half century of active cellular automaton study, rigorous results have been hard to come by. A few exactly solvable models such as the XOR rules (e.g., “Pascal's Triangle mod 2”) have been studied in great detail, especially in one dimension [Garz], [Jen], [Lin]. Some progress has been made in the formal understanding of rather abstract aspects such as symbolic dynamics, and algorithmic decidability (e.g., [Dura], [Har], [Kar], [Pap]). But there are few theorems and proofs which capture precisely the long-term behavior of specific rules. A general theory is out of the question since a Turing machine can be embedded in a CA [Ban], [LN], [Mart], while examples as “simple” as Conway's Life are capable of universal computation. Even the most basic parameterized families of CA systems exhibit a bewildering variety of phenomena: self-organization, metastability, turbulence, self-similarity, and so forth. From a mathematical point of view, cellular automata may rightly be viewed as discrete counterparts to nonlinear partial differential equations. As such, they are able to emulate many aspects of the world around us, while at the same time being particularly easy to implement on a computer. The downside is their resistance, for the most part, to traditional methods of deductive analysis.

Our goal in this paper is to present a mathematical overview of one particular CA topic: the theory of growth and asymptotic shape. We will restrict attention to systems on  $\mathbb{Z}^2$ , the two-dimensional integers, in which each lattice site is either *empty* (0) or *occupied* (1), and in which the set  $A_t$  of occupied sites at time  $t$  grows and attains a limiting geometry. Such *growth models* are interesting in their own right, but also have application to more general dynamics such as models for excitable media [GHH], [FGG1] and crystals [Pac], in which they capture the speed and shape of wave propagation. We will first describe our increasingly detailed rigorous analysis of the best-behaved rules, the *Threshold Growth* models. Next, we examine some simple growth rules with more complex iterates which can nevertheless be determined by a combination of computer experimentation and exact recursion. Then we turn to some rules with behavior so exotic that, at least for now, empirical study seems the only avenue to understanding. We hope that this mix of methods will effectively indicate the current state of knowledge on the subject, and that the exercises and open problems we present will foster further research.

Let us begin with some general notation for CA models. At each successive time step, the sites of  $\mathbb{Z}^2$  become occupied or vacant according to the configuration in their neighborhoods. Thus, let  $0 \in \mathcal{N} \subset \mathbb{Z}^2$  be a prescribed finite neighborhood of the origin, so that its translate  $\mathcal{N}^x = x + \mathcal{N}$  is the neighborhood of site  $x \in \mathbb{Z}^2$ . Sites in  $\mathcal{N}^x \setminus \{x\}$  are called *neighbors* of  $x$ . Introduce the configuration space  $\Xi = \{0, 1\}^{\mathbb{Z}^2}$ , and for  $\xi \in \Xi$ , let  $\xi|_{\Lambda} \in \{0, 1\}^{\Lambda}$  denote the restriction of configuration  $\xi$  to the set  $\Lambda \subset \mathbb{Z}^2$ . A *cellular automaton rule*  $\mathcal{T}$  is a mapping on  $\Xi$  such that  $\mathcal{T}\xi(x) = \mathcal{T}\eta(y)$  whenever  $\xi|_{\mathcal{N}^x - x} = \eta|_{\mathcal{N}^y - y}$ . In words, sites  $x$  and  $y$  use the same update rule whenever they “see” the same local configuration in their respective neighborhoods. Let  $\xi_t(x) \in \{0, 1\}$  be the state at site  $x$  at time  $t$ ,  $\xi_t$  the system as a whole. As is customary, we will often think of the CA as a set-valued process, confounding  $\xi_t$  with  $\{x: \xi_t(x) = 1\}$ . For instance, this allows us to write  $\xi_t^{A_0} = \mathcal{T}^t A_0 = A_t$  to mean that starting from configuration  $\xi_0 = A_0$  we arrive at the set  $A_t$  of occupied sites after  $t$  iterations of rule  $\mathcal{T}$ .

For convenience, this paper will focus on *range  $\rho$  box neighborhoods*:  $\mathcal{N} = B_\rho = \{y \in \mathbb{Z}^2 : \|y\|_\infty \leq \rho\}$  ( $\rho \geq 1$ ), and almost all of our case studies will have  $\rho = 1$ , with (“Moore”) neighbors conveniently described as  $\{N, S, E, W, NE, SE, NW, SW\}$ . Henceforth, let us abbreviate the size of the neighbor set as  $N = |\mathcal{N}| = (2\rho + 1)^2$ . We also restrict attention to *totalistic* automata, in which the update rule depends only on a cell's state and the *number* of its occupied neighbors, but not on the arrangement of those neighbors. Thus there are maps  $\beta, \sigma : \{0, 1, \dots, N - 1\} \rightarrow \{0, 1\}$  such that

$$(1.1) \quad \xi_{t+1}(x) = \begin{cases} 1 & \text{if } \xi_t(x) = 0 \text{ and } \beta(|A_t \cap \mathcal{N}^x|) = 1 \\ & \text{or} \\ & \text{if } \xi_t(x) = 1 \text{ and } \sigma(|A_t \cap \mathcal{N}^x| - 1) = 1; \\ 0 & \text{otherwise} \end{cases}$$

That is to say, a *birth* occurs at  $x$  when it “sees” a number of occupied neighbors in the support of  $\beta$ , while the cell at  $x$  *survives* if the number of occupied neighbors is in the support of  $\sigma$ .

Equivalently, as a map on subsets of  $\mathbb{Z}^2$ ,

$$\mathcal{T}(A) = \{x \in A^c : \beta(|A \cap \mathcal{N}^x|) = 1\} \cup \{x \in A : \sigma(|A \cap \mathcal{N}^x| - 1) = 1\}.$$

Starting from a finite “seed”  $A_0$ , the CA evolution is determined by iteration:  $A_{t+1} = \mathcal{T}(A_t)$ .

Although Conway's Game of Life and some of its variants have been studied extensively since the 1970's, the first systematic empirical investigation of nearest-neighbor totalistic CA rules was carried out during the early 1980's in a series of influential papers by Wolfram [Wol1] which dealt mainly with one-dimensional systems. For our purposes, the most relevant reference is a fascinating experimental survey of two-dimensional cellular automata by Packard and Wolfram [PW] from 1985. They called the  $2^{18}$  Moore neighborhood rules of form (1.1) *outer totalistic*, labeling them in terms of the index:

$$\sum_{i=0}^8 (\beta(i)2^{2i} + \sigma(i)2^{2i+1}).$$

For instance, Conway's Life is Rule 224, and XOR on  $B_1$  is Rule 157,286 . Since this taxonomy is not particularly enlightening, we will choose more descriptive names for the CA rules discussed here.

Among the provocative findings in [PW] are this summary of the shapes observed:

*“Most two-dimensional patterns generated by cellular automaton growth have a polytopic boundary that reflects the structure of the neighborhood in the cellular automaton rule. Some rules, however, yield slowly growing patterns that tend to a circular shape independent of the underlying cellular automaton lattice.”*

this concerning dependence on the initial configuration:

*“... the growth dimensions for the resulting patterns are usually independent of the form of the initial seed. ... There are nevertheless some cellular automaton rules for which slightly different seeds can lead to very different patterns.”*

and this on CA complexity:

*“Despite the simplicity of their construction, cellular automata are found to be capable of very complicated behavior. Direct mathematical analysis is in general of little utility in elucidating their properties.”*

In keeping with this last sentiment, nowhere in [PW] do the authors explain exactly what is meant by a growth rule or its asymptotic shape. Nor do they offer any compelling evidence for the claim that CA growth can become increasingly circular. In order to discuss such intriguing phenomenological issues, it is illuminating (and reasonably straightforward) to adopt a precise framework and terminology for systems  $\xi_t$  which evolve from a finite initial set  $A$  of occupied sites.

For maximum flexibility, we will call  $\xi_t$  a *growth model* as long as  $\beta(0) = 0$ , in which case 1's cannot appear spontaneously in a sea of 0's, instead arising only by local “contact” with other occupied cells. In case  $\sigma(N - 1) = 1$ , so that 0's can only arise by interaction at the edge of the growth cluster, we say that  $\xi_t$  is an *interfacial* growth model. Particularly simple are the *solidification* models with  $\sigma \equiv 1$ , in which any site is permanently occupied once a birth occurs there. Two additional structural properties facilitate mathematical analysis. First, a few cellular automata are *linear*, or *additive*, meaning they satisfy the superposition property

$$(1.2 a) \quad \xi_t^{A_1 \Delta A_2} = \xi_t^{A_1} \Delta \xi_t^{A_2} \quad \text{for all } t \geq 0,$$

(where  $\Delta$  denotes symmetric difference), or

$$(1.2 b) \quad \xi_t^{A_1 \cup A_2} = \xi_t^{A_1} \cup \xi_t^{A_2} \quad \text{for all } t \geq 0,$$

respectively. Equivalently, these are the *XOR* processes such that

$$\xi_1^A(x) = |A \cap \mathcal{N}^x| \pmod{2},$$

which in the range 1 box case has  $\beta = 1_{\{1,3,5,7\}}$  and  $\sigma = 1_{\{0,2,4,6,8\}}$ , and *OR* processes such that

$$\xi_1^A(x) = 1_{A \cap \mathcal{N}^x \neq \emptyset},$$

which in the range 1 box case has  $\beta = 1_{\{1,\dots,8\}}$  and  $\sigma \equiv 1$ . A larger, but still quite restrictive class of automata are *monotone (attractive)*, meaning that whenever  $A_1 \subset A_2$ ,

$$(1.3) \quad \xi_t^{A_1} \subset \xi_t^{A_2} \quad \text{for all } t > 0.$$

Note that CA growth models are monotone if and only if  $\beta$  and  $\sigma$  are both non-decreasing and  $\beta \leq \sigma$ , meaning that the maps jump to value 1 at thresholds  $\theta_0, \theta_1$ , with  $0 \leq \theta_1 \leq \theta_0 \leq N$ .

The notion of limiting shape is easiest to conceptualize for solidification models. In that case  $\xi_t(x)$  may change at most once for each  $x$ , so we let  $\xi_\infty(x)$  denote the eventual state. The set  $A_\infty = \{x : \xi_\infty(x) = 1\}$  then equals  $\bigcup_t A_t$ . Of course this limit may be some finite final crystal (*fixation*), or conceivably some complex infinite dendritic formation. But one expects most rules capable of growth (roughly, the “supercritical” ones) to fill  $\mathbb{Z}^2$  in an orderly fashion, and to spread out linearly in time with a characteristic shape when started from sufficiently large (again, “supercritical”) seeds. With this scenario in mind, say that a CA has asymptotic shape  $L$  started from  $A_0$  if

$$(1.4) \quad t^{-1}A_t \xrightarrow{H} L,$$

where  $\xrightarrow{H}$  denotes convergence in the Hausdorff metric. (Every point in the set on the left is eventually within distance  $\epsilon$  of the set on the right, and vice versa.) Of course there is no guarantee that the occupied set of a particular CA will spread at a linear rate, or even if it does that the geometry of its growth will converge in the sense of (1.4), but such behavior is widely observed in computer experiments and

confirmed by the rigorous results for Threshold Growth and other tractable rules to be discussed in this paper. New complications arise when we attempt to formulate shape results for models in which occupied sites can become empty. Even in well-behaved dynamics, one then expects the occupied region to exhibit a dynamic “pattern” as it spreads. As long as this pattern has positive density, the limit in (1.4) may still be expected to exist, but  $L$  will capture only the shape of the growth, not its characteristic density. We will formulate a refinement of (1.4) which incorporates a density profile when this issue arises in Section 3.

The organization of the remainder of the paper is as follows. We begin in Section 2 by reviewing our current understanding of *Threshold Growth*: monotone solidification models ( $\theta_1 = 0; \theta_0 = \theta$ , a parameter) for which a reasonably complete theory is available. The limit (1.4) holds in full generality, there is an explicit formula for the asymptotic  $L$  in terms of the system's threshold  $\theta$ , and subtler issues of nucleation from small seeds can be analyzed in some detail. For comparison with more general models, let us state the basic Shape Theorem in some detail:

**Theorem 1.** *For Threshold Growth with a box neighborhood, starting from any finite initial seed  $A_0$  such that  $A_\infty = \mathbb{Z}^2$ ,*

- (i) *the occupied set  $A_t$  spreads out linearly in time  $t$ ;*
- (ii)  *$t^{-1}A_t$  attains a limiting shape  $L$ ;*
- (1.5) (iii)  *$L$  is independent of the initial seed  $A_0$ ;*
- (iv)  *$L$  is convex;*
- (v)  *$L$  is a polygon.*

We will describe three methods of proof: *direct recursion*, which can be used for rules with small range; convex analysis, which describes  $L$  as a certain polar transform (Wulff shape, cf. [TCH]); and the more robust *subadditivity* approach, which applies to a great many monotone spatial systems, but yields only an implicit representation of the asymptotic shape. A simple extension shows that monotone growth models obey the same theorem, with the same limit  $L$ , independent of  $\theta_1$ . The section concludes with a brief discussion of *nucleation* questions: which small seeds manage to grow and which do not.

In Sections 3-6 we present a series of examples to demonstrate that in CA growth models which are nonmonotone, any and all of (i) - (v) above may fail. Since cellular automata are capable of universal computation, any kind of growth can be concocted within the general CA framework. However this observation is of little use in understanding how items (i) - (v) fare within our rather restrictive class of growth models. Section 3 begins an exploration of arguably the simplest nonmonotone rules on the

Moore neighborhood. We first examine *Biased Voter Automata*, growth models having arbitrary birth and survival thresholds  $\theta_0, \theta_1$ , in which case more exotic scenarios such as concentric rings and nonconstant limiting density profiles arise. We then turn to *Exactly  $\theta$  Growth Automata* in which a site is permanently added to the occupied set the first time it has exactly  $\theta$  occupied neighbors. For  $\theta = 1$  we find that starting from  $A_0 = \{0\}$ , a crystal with oscillating von Koch type boundary evolves. In particular, (1.4 *ii*) only holds along suitable subsequences, with a distinct limit along each  $t_n = \alpha 2^n, \alpha \in [\frac{1}{2}, 1)$ . The case  $\theta = 2$  provides another example of CA growth with complex boundary dynamics. It is easy to check that any  $2 \times n$  box  $A_0$  grows, but apart from the  $2 \times 2$  case one must resort to computer realizations in order to investigate the apparent limit  $L$  and whether it equals the full diamond  $\mathcal{D} = \{x \in \mathbb{R}^2 : \|x\|_1 \leq 1\}$ .

Section 4 treats the *Exactly 3 CA*, one of the most exotic of all growth rules, which generates remarkable complexity but seems amenable to some interesting experimental mathematics. This is Conway's Game with no  $1 \rightarrow 0$  transitions, so it is called *Life without Death (LwoD)*. One encounters dendritic “icicle” growth patterns that produce a seemingly stochastic mix: chaotic crystalline *lava*, horizontal and vertical *ladders* which evolve by a kind of weaving pattern and seem to outrun the surrounding lava, and parasitic *shoots* which emerge from the lava but can only race along the edges of ladders. The resulting interactions give rise to large-scale self-organization in which extensive regions of the growing crystal are repeatedly cloned *exactly* in time. As an indication that LwoD  $A_t$  can be analyzed mathematically, we will prove one result which captures its *sensitive dependence on initial conditions*. Namely, given *any* finite initial configuration  $A_0$ , one can produce configurations  $C_1$  and  $C_2$  each consisting of at most 28 cells, such that  $A_t$  grows persistently starting from  $A_0 \cup C_1$ , but fixates starting from  $A_0 \cup C_2$ . The ability of LwoD to emulate arbitrary Boolean circuits is also discussed briefly.

Next, in Section 5, we turn to solidification automata in which a birth occurs if either  $\theta$  or  $\theta'$  of the 8 neighbors are occupied. Various rules with  $\theta = 2$  and 3 provide “counterexamples” to several parts of Shape Theorem (1.5). Recursive dynamics establish that the limit  $L$  can depend on the initial seed  $A_0$ , and be nonconvex in certain cases. There is also an example of *sublinear* persistent growth from a suitable  $A_0$ . Computer experiments seem to suggest that some examples with chaotic boundary dynamics have limit shapes with piecewise smooth boundary, while others remain asymptotically polygonal. But one must be quite careful in reaching conclusions based on visualization – we will mention one case which seems to indicate an octagonal  $L$  for the first several hundred updates but later is more suggestive of a shape with smooth boundary.

Section 6 presents empirical case studies for three of the most intriguing CA growth models of all. *Wolfram's Crystal* is the nearest neighbor totalistic rule which seems to do as good a job as any of spreading like a circle. We present numerical data concerning the first several thousand updates of its

evolution from a small lattice circle, interpreting the results in the context of the general *isotropy problem* for local spatial growth dynamics. Our second gem is *Hickerson's Diamoeba*, the most volatile interfacial growth model we know. We will exhibit arbitrarily large seeds from which  $A_t$  dies out completely, whereas experiments show that comparatively small seeds with slight lattice asymmetry can grow to fill an array several thousand cells on a side. One thus suspects that persistent growth is possible. However boundary shocks are so catastrophic, and ultimate growth so tenuous, that the prospects for a limit shape  $L$  remain decidedly murky. Then we turn to *Conway's Life*. This renowned CA continues to be studied intensively after more than 25 years of avid experimentation and analysis. Indeed, there have been major breakthroughs in the design of recursive organizing seeds for Life within the past few years. Still, many of the most basic ergodic properties of the rule remain a mystery. We survey the current state of knowledge, with an emphasis on growth-related issues.

Finally, in Section 7 we present a brief overview of *stochastic growth* – in cellular automata which evolve from random initial states, and also for processes which evolve randomly. With deterministic updating, chance enters the picture when we start from a random set, e.g. from the Bernoulli product measure  $\mu_p$  which occupies each site in  $\mathbb{Z}^2$  independently with probability  $p > 0$ . Such CA rules from random initial states *are* stochastic processes, albeit degenerate, and are among the most mathematically tractable prototypes for various nonlinear spatio-temporal phenomena. For random spatial dynamics such as interacting particle systems [Lig], [Durr], problems of asymptotic shape have played a central role since Eden's crystal growth model [Ede] and Broadbent and Hammersley's first-passage percolation [BH] were introduced in the late 1950s. The boundary interface of even the simplest random dynamics exhibit complex fluctuations, making explicit determination of  $L$  exceedingly difficult. Thus subadditivity is often the only available technique for proving shape theorems. Until now, some variant of the additivity property (1.2b) has been a key assumption. We describe a new result of type (1.4) for randomized CA dynamics called Stochastic Threshold Growth, due to Bohman and Gravner [BG]. Their analysis of these nonlinear systems relies on a deterministic combinatorial lemma which extends the regularity theory for Threshold Growth CA models recently developed by Bohman [Boh]. Finally, we show how it is possible to estimate  $L$  efficiently by Monte Carlo simulation, and thereby present evidence for an intriguing *convexification transition* as the random component of the dynamics increases.

Numerous problems are posed throughout the paper. Some are intended as exercises, others as avenues for further research. Also, our introductory discussion makes it clear that computer calculation and visualization play an indispensable role in the study of cellular automaton growth. Most of the experiments in this paper were performed using our own *WinCA* [FG] software; [GN] provides an alternative based on *Mathematica*. The paper concludes with an Appendix listing additional electronic resources available to the reader: links to the World Wide Web, downloadable computer programs, and a library of companion CA experiments for this research, available on various platforms.



## 2. Threshold and Monotone Growth

We begin our survey with the most tractable CA growth models, the monotone solidification rules in which an empty cell joins the occupied set iff it sees enough occupied sites around it.. Reiterating notation from the Introduction, let  $0 \in \mathcal{N} \subset \mathbb{Z}^2$  be a *neighborhood* of the origin, and let  $\theta$ , a positive integer, be the *threshold*. We will assume  $\mathcal{N}$  symmetric for simplicity, focusing on the range  $\rho$  box neighborhood case  $\mathcal{N} = B_\rho = \{x : \|x\|_\infty \leq \rho\}$ . Given  $A \subset \mathbb{Z}^2$ , define

$$(2.1) \quad \mathcal{T}A = A \cup \{x : |\mathcal{N}^x \cap A| \geq \theta\}.$$

Start from  $A_0 \subset \mathbb{Z}^2$  and iterate,  $A_{t+1} = \mathcal{T}A_t$ , to generate *Threshold Growth*. Recall the equivalent coordinate notation  $\xi_t^{A_0} = \mathcal{T}^t A_0 = A_t$ .

Such models are naturally classified according to whether or not they are capable of filling the lattice eventually. Since (2.1) is a solidification rule,  $A_\infty = \lim_n A_n$  exists. Call  $A_n$  *supercritical* if  $A_\infty = \mathbb{Z}^2$  for some finite  $A_0$ , *subcritical* if  $A_\infty \neq \mathbb{Z}^2$  for some  $A_0$  with finite complement, and *critical* otherwise. For symmetric  $\mathcal{N}$  one can give a complete classification. Denote  $\iota(\mathcal{N}) = \max\{|\mathcal{N} \cap \ell| : \ell \text{ a line through } \mathbf{0}\}$ . Then it turns out ([GG2]) the dynamics are

$$(2.2) \quad \begin{array}{ll} \text{supercritical} & \text{iff} \quad \theta \leq \frac{1}{2}(|\mathcal{N}| - \iota(\mathcal{N})), \\ \text{subcritical} & \text{iff} \quad \theta > \frac{1}{2}(|\mathcal{N}| - 1). \end{array}$$

In the range  $\rho$  box case, these cutoffs are  $2\rho^2 + \rho$  and  $2\rho^2 + 2\rho$ , respectively. The crux of the first equivalence in (2.2) is to show that a sufficiently large lattice ball fills  $\mathbb{Z}^2$  as long as the threshold is appreciably less than half the size of the neighbor set.

To motivate the discussion of asymptotic shape for Threshold Growth, consider our

$$\textit{Basic Example: } \mathcal{N} = B_1, \theta = 3.$$

Note that this is the Moore neighborhood rule with highest supercritical threshold. From a suitably large seed  $A_0$ , say any configuration containing 3 cells in a row,  $A_t$  rapidly forms a linearly expanding “lattice octagon,” so (1.4) holds with  $L = \mathcal{O}$ , the octagonal region bounded by vertices  $(\pm \frac{1}{2}, 0)$ ,  $(0, \pm \frac{1}{2})$ ,  $(\pm \frac{1}{3}, \pm \frac{1}{3})$ . The most straightforward route to Theorem 1 for specific rules is to compute iterates exactly. In our case, starting from the range 1 diamond seed  $D_1 = \{\|x\|_1 \leq 1\}$ , it turns out that

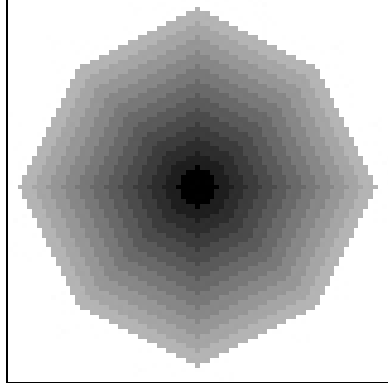
$$(2.3) \quad \mathcal{T}^t D_1 = \{(x_1, x_2) : \max[|x_1| + 2|x_2|, 2|x_1| + |x_2|] \leq t + 2\}.$$

Fig.1a shows each 6 updates in a new shade of gray. One can verify (2.3) by induction, checking the first few iterates directly and then observing that the “sides” of the lattice octagons advance like boundaries of

half-spaces:

$$\{x_1 + 2x_2 \leq t\} \rightarrow \{x_1 + 2x_2 \leq t + 1\},$$

whereas the “corners” advance with period 2 (horizontal, vertical) and 3 (diagonal; see Fig. 1b).



**Fig. 1a.**  $\mathcal{T}^{6n}D$ ;  $n = 1, \dots, 12$

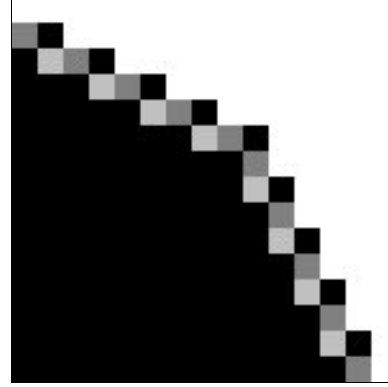


**Fig. 1b.** Detail of a stable corner

Convergence to  $\mathcal{O}$  follows immediately from (2.3). Next, given any finite  $A_0$  for which  $A_\infty = \mathbb{Z}^2$ , choose  $n$  so that  $D_1 \subset \mathcal{T}^n A_0$  and  $A_0 \subset \mathcal{T}^n D_1$ . Monotonicity (1.3) yields  $\mathcal{T}^t D_1 \subset \mathcal{T}^{t+n} A_0 \subset \mathcal{T}^{t+2n} D_1$ , so (1.4) holds with  $L = \mathcal{O}$ , establishing Theorem 1 for our Basic Example.

With larger neighborhoods and thresholds exact recursion becomes increasingly difficult, so an alternate method is needed in order to establish the Shape Theorem for Threshold Growth in full generality. An approach familiar to statistical physicists ([DKS], [KrSp]) is based on *half-space propagation*. Roughly, the idea is that any expanding droplet should become locally flat as it grows, and so its displacement in direction  $\alpha$  is determined by the advance of a half-space  $H_u^- = \{x \cdot u \leq 0\}$ , where  $u$  is the outward normal unit vector to the boundary of  $A_t$  in direction  $\alpha$ . After some convex analysis [GG1], the recipe is essentially as follows. By translation invariance,  $\mathcal{T}(H_u^-) = H_u^- + w(u)u$  for some function  $w(u)$  known as the *speed*. From this computable data, form the region of  $\mathbb{R}^2$  with extent  $w^{-1}$ ,

$$K = K_{1/w} = \bigcup_u [0, 1/w(u)]u .$$

Then the asymptotic shape  $L$  is given by the polar transform of  $K$ ,

$$(2.4) \quad L = K^* = \{x : x \cdot y \leq 1 \text{ for every } y \in K_{1/w}\}.$$

Let's see how the formalism works for our Basic Example. In this case it turns out that  $K$  is a nonconvex 16-gon (Fig. 2), with vertices  $(1,0)$ ,  $(2,1)$ ,  $(1,1)$ , and 13 more dictated by the symmetries of the lattice. For instance, the diagram reflects the fact that while horizontal and vertical half-spaces advance with speed 1, a half-space with slope 2 only advances at speed  $\frac{1}{\sqrt{5}}$ . Despite the nonconvexity, one gets  $K^* = \mathcal{O}$  (the small dark octagon in Fig. 2), which we have already shown to be the asymptotic

shape  $L$ . For polygonal  $K$  one can obtain the *shape* (but not the size) of  $L$  geometrically by forming the intersection of half-spaces containing the origin and normal to vectors  $v$  which end at a vertex of the convex hull of  $K$ . This intersection is the white octagon in Fig. 1. Since the limit set (2.4) can also be represented as

$$L = \bigcap_u (w(u)u + H_u^-),$$

the size is then determined by a half-space velocity corresponding to one of the polygonal sides.

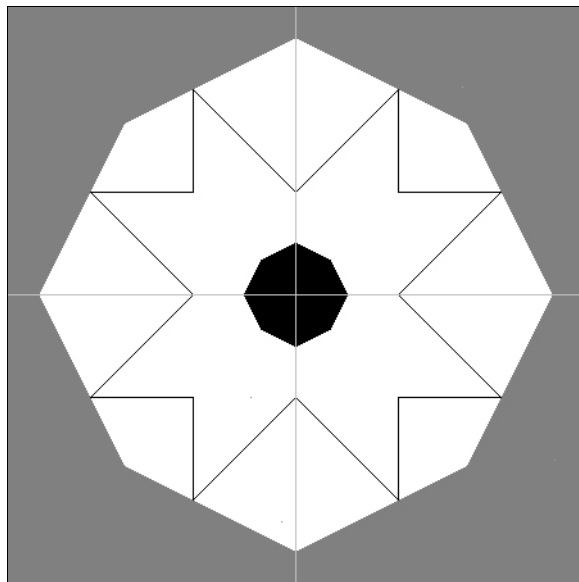


**Fig. 2.**  $K$  for range 1 box,  $\theta = 3$

Evidently (2.4) is valid for our Basic Example even though the boundary of  $\mathcal{O}$  is not smooth so that the heuristics leading to the polar representation break down. In fact, formula (2.4) is *always* valid for Threshold Growth, and establishes Theorem 1 in full generality. A careful analysis relies on conjugate dynamics  $\overline{\mathcal{T}}$  on  $\mathbb{R}^2$ , needed to define  $w$  properly, such that

$$\overline{\mathcal{T}}(A) \cap \mathbb{Z}^2 = \mathcal{T}(A \cap \mathbb{Z}^2).$$

With this trick one can mimic the technology of Euclidean Threshold Growth; [GG1] and [GG2] provide the details, including an argument that  $L$  is always a polygon. See [Wil1] for another proof of Theorem 1.

According to (2.2), there are 10 supercritical polygonal limit shapes for  $\mathcal{N} = B_2$ , corresponding to thresholds  $1, \dots, 10$ . Fig. 2 of [GG2] shows them all as overlays when the successive dynamics are run from a suitable small initial seed. Clearly, smaller polygons correspond to larger thresholds, but the number of sides varies irregularly: 4, 8, 8, 12, 8, 12, 4, 4, 8, 8. Curiously, the limits  $L$  are identical for  $\theta = 7$  and  $\theta = 8$ . As  $\rho, \theta \rightarrow \infty$ , in such a way that  $\theta/\rho^2 \rightarrow \lambda \in [0, 2]$ , the limit shape  $L_{\rho, \theta}$  for  $\mathcal{N}_\rho$  and

threshold  $\theta$  converges to a convex  $L_\lambda$  with piecewise smooth boundary which is described in [GG1]. In spite of formula (2.4), we do not know how the number of polygonal sides grows with  $\rho$ . Thus, we pose

**Problem 1.** As  $\rho \rightarrow \infty$ , determine the asymptotic growth rate for the maximal number of sides of  $L_{\rho,\theta}$ ;  $1 \leq \theta \leq 2\rho^2 + \rho$ .

Another approach to asymptotic shape for monotone dynamics exploits *subadditivity*: the fact that growth accelerates as additional sites become occupied. More precisely, for any initial seed  $A_0$  which fills  $\mathbb{Z}^2$  eventually, and any site  $x$ , let  $\tau(x)$  denote the time until  $\xi_t$  occupies  $x$  starting from  $A_0$ . Suppose that once a sufficiently distant  $x$  is occupied, it must be the case that  $x + A_0$  is totally covered after  $r$  additional updates, where  $r$  is independent of  $x$ . Then for any  $x, y \in \mathbb{Z}^2$ ,

$$(2.5) \quad \tau(x + y) \leq \tau(x) + \tau(y) + r,$$

since by (1.3) it can take no longer than  $\tau(y)$  additional updates for the configuration covering  $x + A_0$  at time  $\tau(x) + r$  to reach site  $x + y$ . Extend  $\tau$  to all of  $\mathbb{R}^2$  by identifying each site of the lattice with the unit cell centered at that site, adopting some convention along cell edges. Set  $v(x) = \inf_n n^{-1}\tau(nx)$ ,  $x \in \mathbb{R}^2$ . It follows from (2.5) that  $n^{-1}\tau(nx) \rightarrow v(x)$  as  $n \rightarrow \infty$ , that  $v(x)$  defines a norm, and that (1.4) holds with the convex limit shape given implicitly as the unit ball

$$(2.6) \quad L = \{x : v(x) \leq 1\}.$$

One uses monotonicity to show uniqueness of the limit starting from sufficiently large seeds, just as in our recursive proof of Theorem 1 for the Basic Example. This line of argument was first applied about 25 years ago in the context of *random* spatial interactions by D. Richardson [Ric]; Section 7 will discuss the method in more detail. Note, however, that the subadditivity approach does *not* show that  $L$  is a polygon, nor does it give any geometric information other than convexity and lattice symmetry.

For now, let us discuss the method's applicability to Threshold Growth models, in which case we need only manufacture a suitable  $A_0$  and  $r$  leading to (2.5). For our Basic Example it turns out that one can take  $A_0 = B_1$  and  $r = 4$  as long as  $x \notin B_2$ , so (1.4) follows. To see this, first observe that the crystal started from  $B_1$  covers  $B_2$  after two updates. By monotonicity,  $A_{2t}$  covers  $B_t$ , and hence the process fills  $\mathbb{Z}^2$ . We formalize the choice of  $r$  as a lemma, since it will be used again in Section 7 for an extension to random dynamics.

**Lemma.** Let  $x \in A_t$  be any site separated from  $A_0$  by  $\ell^\infty$ -distance at least 2. Restrict the occupied set and the dynamics to  $x + B_2$  from time  $t$  on. Such dynamics will cover  $\mathcal{N}^x$  at time  $t + 4$ .

**Proof.** Clearly  $A_{t-1}$  must contain 3 neighbors of  $x$ . Unless those 3 occupied sites comprise a corner cell and its two adjacent neighbors (other than  $x$ ), it is straightforward to check that  $A_{t+3}$  covers  $x + B_1$  using only the dynamics restricted to that neighborhood. If the 3 sites lie in a corner, and  $x \notin A_1$ , then some neighbor of one of the 3 sites (other than  $x$ ) must have been occupied at time  $t - 2$ . In this case one can check that  $A_{t+4}$  covers  $\mathcal{N}^x$  using only the dynamics restricted to  $x + B_2$ .  $\square$

Of course, carrying out such explicit case checking for larger ranges and thresholds rapidly becomes unmanageable, even with the aid of a computer. In order to describe the subadditivity approach to general supercritical Threshold Growth, we digress briefly and consider some delicate combinatorial questions connected with *nucleation*: Which  $A_0$  manage to grow, and what is the mechanism for initial stages of growth? Here and throughout the remainder of the paper, we say

$$A_0 \text{ generates persistent growth if } |A_t| \rightarrow \infty \text{ as } t \rightarrow \infty,$$

and call the dynamics *omnivorous* if for every  $A_0$  which generates persistent growth,  $A_t \uparrow \mathbb{Z}^2$ .

T. Bohman has recently proved

**Theorem 2. [Boh]** Threshold Growth with neighborhood  $B_\rho$  is omnivorous for any (supercritical)  $\theta$ .

Bohman's proof uses clever “energy” estimates, taking about 2 journal pages for the case  $\theta \leq \rho^2$ , and much longer for general  $\theta \leq \rho(2\rho + 1)$ . The latter part of his analysis depends on the geometry of squares, so it is unclear to which other neighborhoods the result generalizes. At least if  $\mathcal{N} = B_\rho$ , the details of the construction also show that for any  $A_0$  which generates persistent growth, for any  $\sigma < \infty$ , and  $x$  large, there is an  $r = r(\rho, \theta, \sigma)$  such that

$$x + B_\sigma \subset A_{\tau(x)+r},$$

which suffices to prove (1.4) by subadditivity, with  $L$  as in (2.6). Note that Theorem 2 also strengthens Theorem 1, implying that growth started from *any* finite seed either stops eventually or attains asymptotic shape  $L$ .

A simple observation extends that Theorem 1 to any monotone growth model on  $B_\rho$  parameterized by survival and birth thresholds  $\theta_1 \leq \theta_0$ , with  $L = L_{\rho, \theta_0}$ , the corresponding Threshold Growth shape. Namely, choose a large  $A$  so that each of its sites  $x$  sees at least  $\theta_0$  occupied sites (i.e.,  $|B_\rho^x \cap A| \geq \theta_0$ ). For instance, a large lattice ball has this property as long as  $(B_\rho, \theta_0)$  is supercritical. Then at time 1, starting from  $A$ , all occupied sites survive since  $\theta_1 \leq \theta_0$ , and all newly born sites see at least  $\theta_0$  occupied sites by definition of the dynamics. In particular, the new configuration agrees with that of  $(B_\rho, \theta_0)$  Threshold Growth after one update started from  $A$ . Iterating, we see that the dynamics agree with Threshold Growth at all times, so the asymptotic shape is the same. By monotonicity, the Shape Theorem holds for any larger seed.

We conjecture that any box neighborhood monotone rule, started from any finite seed, either fixates or eventually fills  $\mathbb{Z}^2$ . However, the extension of Bohman's result is not immediate, so such rules might conceivably be able to fill in a periodic or an irregular infinite subset of the lattice.

**Problem 2.** Let  $A_t$  be a monotone growth model with Moore (or  $B_\rho$ ) neighborhood. Are periodic finite configurations possible? If the process generates persistent growth, must it be omnivorous?

By contrast, even the simplest nonmonotone rules can exhibit surprising behavior. Our next problem, which requires *WinCA* [FG], or similar CA software, drives home this point.

**Problem 3.** Consider the Biased Voter Automaton on  $\mathcal{N} = B_2$ , with  $\theta_0 = 6$ ,  $\theta_1 = 26$ . Thus, a cell becomes occupied if at least 6 of its 25 range box neighbors are previously occupied, whereas occupied cells automatically become empty. (Thus, the birth and survival maps  $\beta$  and  $\sigma$  are both non-decreasing.) Investigate this model's crystal growth starting from the seeds  $D_6 \subset B_6$ , where  $D_6$  denotes the 6-diamond  $\{\|y\|_1 \leq 6\}$  and  $B_6$  is the 6-box.

Before continuing with the central theme of shape theory in the next Section, we mention some additional nucleation problems about the very smallest seeds which grow. Let  $\gamma = \gamma(\mathcal{N}, \theta)$  be the minimal number of sites needed for persistent growth, and let  $\nu = \nu(\mathcal{N}, \theta)$  be the number of seeds of size  $\gamma$  which generate persistent growth and have their leftmost lowest sites at the origin. Parameters  $\gamma$  and  $\nu$  play key roles in the First Passage and Poisson-Voronoi Tiling results we have obtained in [GG2] and [GG3]. For small neighborhoods (box or not), one can determine  $\gamma$  and explicitly enumerate the  $\nu$  minimal droplets with a computer. For instance,  $\gamma(B_3, 5) = 5$  and  $\nu(B_3, 5) = 574,718$ . As a little puzzle, the reader might check that in the threshold 2 case  $\gamma(B_\rho, 2) = 2$  and  $\nu(B_\rho, 2) = 4\rho(2\rho+1)$ . For larger  $\theta$  no such explicit evaluation of  $\nu$  is available for general  $\rho$ ; a table of small cases appears in [GG2].

If  $\theta$  is small, then there are nucleating occupied sets of  $\theta$  cells, the smallest possible size. For instance, if  $\theta \leq \rho^2$ , then *any* size  $\theta$  subset of a  $\rho \times \rho$  box fills that box in one update, and thereafter covers a box of side  $\rho + t - 1$  at each time  $t$ . The smallest example with  $\gamma > \theta$  is range 2, threshold 10, in which case  $B_2$  does not generate persistent growth, so  $\gamma > \theta$ . However the 11 site configuration in Fig. 3 does nucleate,

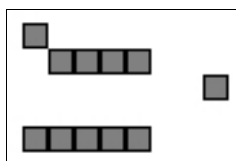


**Fig. 3.** A seed that grows for  $\mathcal{N} = B_2, \theta = 11$

showing that  $\gamma = 11$  in this case. The starting point in understanding  $\gamma$  for large neighborhoods is to demonstrate, for almost every  $\lambda \in (0,2)$ , existence of the threshold-range limit

$$\lim_{\rho \rightarrow \infty} \frac{\gamma(B_\rho, \lambda \rho^2)}{\rho^2} = \gamma^E(\lambda).$$

When  $\lambda$  is small the “design principles” of minimal nucleating droplets are effectively random, but for large  $\lambda$  they become severely constrained. Of particular interest is the largest  $\lambda$  for which  $\gamma^E(\lambda)$  is as small as possible

$$\gamma_c^E = \sup\{\lambda : \gamma^E(\lambda) = \lambda\}.$$

Using interactive visualization to create large-range minimal droplets of size  $\theta$ , as well as related constructions, it is proved in [GG4] that  $1.61 < \gamma_c^E < 1.66$ . Fig. 4 shows level sets of the droplet which yields the lower bound – a range 150 seed consisting of 36,760 cells (white) which grows for  $\theta = 36,760$ . We know of no seed with 36,761 cells that grows for  $\theta = 36,761$ .

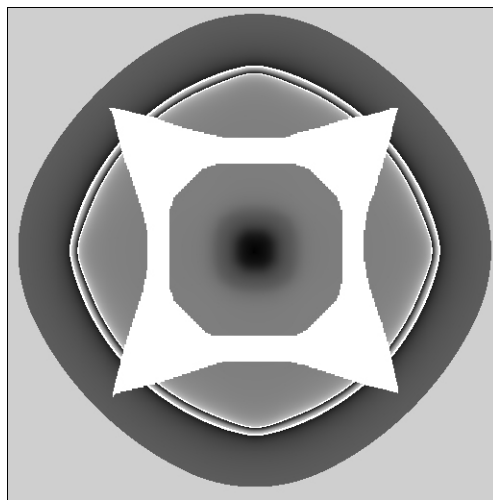


**Fig. 4.** A barely supercritical droplet for range 150 box,  $\theta = 36,760$

### 3. Some Simple Nonmonotone Rules

As we will see shortly, more exotic crystals grow from cellular automaton rules without monotonicity property (1.3). Typically, such rules give rise to chaotic or pseudo-random structure so complicated as to defy mathematical analysis. In rare instances, however, starting from carefully chosen seeds, nonmonotone CA dynamics generate a periodic pattern in space and time which can be spotted by computer visualization and then checked recursively. In this and subsequent sections we present a series of such exactly solvable “counterexamples” in order to show that *all* the regularity properties (1.5 *i* - *v*) of Threshold Growth shape theory may fail in general.

Let us begin with a formalism which may be used to check that a given CA evolves in a prescribed manner. The notation is somewhat burdensome, so we will first describe a simpler setup for solidification rules, then proceed to the general framework.

(3.1) *Recursive specification for solidification rules.*

Assume solidification, i.e., that 1's stay 1's, in which case it is natural to specify growth in terms of sets  $\{\Lambda_n\}_{n \geq 1}$  which partition  $\mathbb{Z}^2$  (i.e., they are disjoint and cover the lattice). They may be thought of as “shells,” regions which contain sites added at successive times. In many cases the discernible pattern of growth is most evident every  $\tau$  updates after some initial epoch  $t_0$ , so let  $t_n = t_0 + n\tau$  be the recursion times, suppose that

$$(i) \quad \mathcal{T}^{t_0}(A_0) = C_0,$$

and for  $n \geq 1$ , let  $C_n \subset \Lambda_n$  designate the set of sites claimed to become occupied at time  $t_n$ . Further partition each “shell”  $\Lambda_n = \bigcup_k \Lambda_n^k$ , write  $\mathcal{N}^\tau = \mathcal{N} + \dots + \mathcal{N}$  ( $\tau$  times), and introduce

$$C_n^k = C_n \cap \Lambda_n^k, \quad \bar{\Lambda}_{n+1}^k = \bigcup_{\ell, m \leq n} [\Lambda_m^\ell \cap (\Lambda_{n+1}^k + \mathcal{N}^\tau)], \quad \bar{C}_{n+1}^k = C_n \cap \bar{\Lambda}_{n+1}^k.$$

The  $(n, k)$  may be thought of as indices for convenient “charts” of the recursive structure – regions of the evolving crystal with a coherent local pattern. Thus,  $C_n^k$  is the designation of occupied sites on chart  $\Lambda_n^k$  at time  $t_n$ .  $\bar{\Lambda}_{n+1}^k$  consists of all those sites which could possibly influence the configuration on chart  $\Lambda_{n+1}^k$  within  $\tau$  updates of the rule  $\mathcal{T}$ , and  $\bar{C}_{n+1}^k$  is the occupied specification on  $\bar{\Lambda}_{n+1}^k$  at time  $t_n$ . Assume also that for each  $k, n$

$$(ii) \quad \mathcal{T}^\tau(\bar{C}_{n+1}^k) \cap \Lambda_{n+1}^k = C_{n+1}^k,$$

and for all  $E \subset (\bigcup_{m \leq n} \Lambda_m)^c$ ,

$$(iii) \quad \mathcal{T}^\tau(\bigcup_{m \leq n} C_m \cup E) \cap (\bigcup_{m \leq n} \Lambda_m) = \bigcup_{m \leq n} C_m.$$

Condition (ii) says that the configuration at time  $t_n$  restricted to a suitable neighborhood of each chart for time  $t_{n+1}$  maps to the specified configuration on that chart after  $\tau$  updates. Condition (iii) ensures that once the configuration on the first  $n$  shells is known to be  $\bigcup_{m \leq n} C_m$  at time  $t_n$ , then no additional set of occupied sites  $E$  added at some later time can possibly change the crystal on those shells.

Consequently, a straightforward induction using (i) – (iii) shows that

$$A_{t_n} = \bigcup_{m \leq n} C_m \text{ for all } n,$$

i.e., the true dynamics of the solidification model agree with its a priori specification.



Let us illustrate this formalism by sketching a few more details of the proof of (2.3) for our Basic Example. There the iterates fill  $\mathbb{Z}^2$  (i.e., there are no permanently vacant sites), so it is natural to choose  $\Lambda_n = C_n$ , in which case solidification guarantees condition (iii). As previously noted, the shapes of the corners have periods 2 and 3, so it is perhaps simplest to take  $\tau = 6$ , and for sufficient “elbow room”  $t_0 = 48$ , say. Then, in light of (2.3), for  $n \geq 1$  we can prescribe

$$\Lambda_n = C_n = \{(x_1, x_2) : 6n + 45 \leq \max[|x_1| + 2|x_2|, 2|x_1| + |x_2|] \leq 6n + 50\},$$

checking directly (by computer!) that  $\mathcal{T}^{48}(D_1) = \{\max[|x_1| + 2|x_2|, 2|x_1| + |x_2|] \leq 50\}$ . Next, we partition each shell  $\Lambda_n$  into suitable charts  $\Lambda_n^k$  which correspond to the sides and corners of the growing octagon. Let the 8 corner charts consist of those sites in  $\Lambda_n$  which are at most  $\ell_\infty$ -distance 6 from each of the coordinate axes and lines  $x_2 = \pm x_1$ . Let the 8 side charts be the connected components of the complementary portion of  $\Lambda_n$ . This decomposition and symmetry effectively reduces the verification of condition (ii) for recursive specification to three cases: sides, and horizontal and diagonal corners. By construction, each chart  $\Lambda_{n+1}^k$  extends in a homogeneous fashion, meaning that the side charts extend consistently with lattice half-spaces while the corners extend consistently with lattice wedges (i.e., intersections of two half-spaces). Thus it suffices to check that the half space  $x_1 + 2x_2 \leq n$  advances to  $x_1 + 2x_2 \leq n + 1$  in one update, which is immediate from the threshold 3 update rule, and to verify that the corner charts advance in keeping with (2.3), each with the same profile after 6 updates. For the diagonal corners this last is ensured by Fig.1. A similar but simpler calculation handles the other corners and completes the verification.

The previous paragraph captures the spirit of our inductive scheme: by decomposing a configuration into homogeneous charts one need only check the claimed behavior of the update rule in a relatively small number of cases rather than at every individual site. In practice, though, symbolic specification is tedious and unenlightening. With effective CA visualization, it is often possible to check directly from a picture or animation that the evolution is recursively specified. For the remainder of the paper we will present our exactly solvable examples via graphics which we hope the reader will find convincing. Use of a friendly interactive CA interface such as *WinCA* [FG] greatly eases the verification.

### A Biased Voter Example

As our first example of nonmonotone growth, we choose a Biased Voter CA with  $\theta_0 < \theta_1$ . Namely, let us consider the range 2 box model with  $\theta_0 = 1$ ,  $\theta_1 = 16$ , starting from a lattice ball of “radius” 7 (about the smallest size which gives rise to the interesting behavior we want to discuss). Throughout this paper; in keeping with *WinCA*, the lattice ball of “radius”  $r$  is taken to be  $\{\|x\|_2 < r + \frac{1}{2}\}$ . Fig. 5 shows the configuration at time 40, suggesting that successive updates fill the plane in a predictable fashion. The totally occupied nonconvex star grows linearly, with a characteristic shape and periodic corners.

Alternating occupied and vacant stripes of constant width 2 fill out the box which circumscribes the star. Each update flips the states on the interior of the striped region, and a new outer occupied ring is added. By carefully eyeballing a few iterates with a program such as *WinCA*, it is easy to see that the dynamics reproduce exactly.

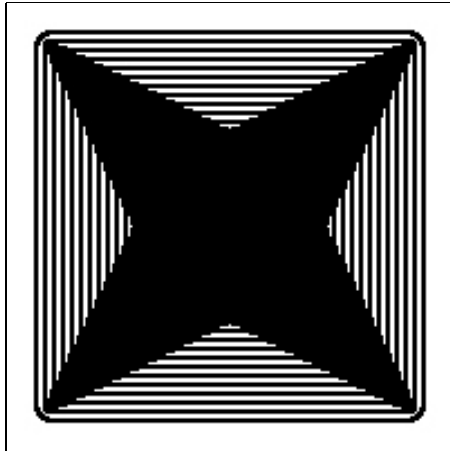


**Fig. 5.** Discontinuous density in the range 2 box  
Biased Voter Automaton,  $\theta_0 = 1$ ,  $\theta_1 = 16$

However this is not a solidification model, so one needs to generalize (3.1). The shells of the simpler scheme must be replaced by arbitrary configurations of the entire lattice, since sites may change state repeatedly. Thus, we partition all of  $\mathbb{Z}^2$  into charts  $\Lambda_n^k$  at each time  $n$ . In place of condition (iii), the more extensive charts must be checked, but otherwise the formalism is the same. Equivalently, one may frame the general case in terms of CA solidification in three-dimensional space-time. See [Toom] for examples of that approach.

### (3.2) Recursive specification for general cellular automata.

$\tau \geq 1$  is the period of recursion;  $t_n = t_0 + n\tau$  are the recursion times.  $\Lambda_n = \{\Lambda_n^k\}$  is a partition of  $\mathbb{Z}^2$  for each fixed  $n$ .  $C_n$  designates the sites which are claimed to be occupied at time  $t_n$ . With the same notation as in (3.1), assume that (3.1 i - ii) hold. Then  $A_{t_n} = C_n$  for all  $n$ .

After a suitable initial time  $t_0$  during which the pattern stabilizes and attains a sufficiently large size, application of (3.2) to our Biased Voter example involves charts of 7 varieties, in order to handle: the interior of the star, the exterior of the box, the interior of the edges of the star, the interior of the edges of the box, the interior of the striped region, the corners of the star/box, and the concave corners of the star. All of these propagate with period 1 or 2, except for the last kind which has period 4. Thus, simple recursive growth is easily verified by computer visualization. So what is the asymptotic shape  $L$  here? Note that the Hausdorff metric in (1.4) does not distinguish between solid coverage and local occupancy with a uniformly positive density. Hence  $L$  agrees with the normalized “light cone,” a Euclidean box  $\mathcal{B}_4$  of side 4, centered at the origin, which represents the largest possible region attainable by range 2

growth. In models which do not fill the lattice completely as they spread, a more detailed *asymptotic density profile* is clearly desirable in order to capture subtler aspects of crystal geometry such as that indicated in Fig.5.

To this end, introduce the measure  $\mu_t$  concentrated on  $A_t/t$ , and assigning mass  $1/t^2$  to each point in the normalized configuration. Let  $\mu$  be a measure on  $\mathbb{R}^2$  with compact support. Then we say that  $t^{-1}A_t \rightarrow \mu$  in measure as  $t \rightarrow \infty$  if  $\mu_t$  converges weakly to  $\mu$ , that is to say

$$(3.3) \quad \int f d\mu_t \rightarrow \int f d\mu \quad \text{for all } f \in \mathcal{C}_c(\mathbb{R}^2).$$

Note that, since the  $\mu_t$  are uniformly bounded and have uniformly bounded support, they have at least one limit point. As we shall see, the number of limit points may be uncountable. We should also observe that while this notion can capture densities other than 1, it also sometimes loses information. For instance, if  $t^{-1}A_t$  converges to a line segment in the Hausdorff metric, then  $t^{-1}A_t$  converges to 0 in measure. One general remark is also in order. Namely, suppose  $\mu$  is any limit point of  $\mu_t$ . Since  $A_t \subset \mathbb{Z}^2$  and  $\mathbb{Z}^2/t$  converges to Lebesgue measure in the above sense, it follows that  $\mu(K) \leq \text{area}(K)$  for any measurable  $K \subset \mathbb{R}^2$ . Hence there is a measurable  $\phi : \mathbb{R}^2 \rightarrow [0, 1]$  such that  $\mu = \phi dx$ . In this sense, we could simply write  $t^{-1}A_t \rightarrow \phi$ .

For our Biased Voter example, let  $\mathcal{S}$  denote the Euclidean star polygon with 4 vertices at  $(0, \pm 1)$  and  $(\pm 1, 0)$ , and 4 vertices at the corners of  $\mathcal{B}_4$ . Then  $A_t/t$  converges in measure to the  $\mu$  which has density 1 on  $\mathcal{S}$ ,  $\frac{1}{2}$  on  $\mathcal{B}_4 \setminus \mathcal{S}$ , and 0 elsewhere. Even for growth models which do not fill the lattice, the most common scenario would seem to be an asymptotic shape with constant local density throughout, i.e.,  $\mu(dx) = c \cdot 1_L(x) dx$  for some  $c > 0$ . Another plausible behavior is a smooth “hydrodynamic” profile over the support of  $L$ . A novel feature in the present case is the abrupt change of density at the boundary of  $\mathcal{S}$ . Additional instances of (3.3) will appear throughout the paper.

Fig. 5 also suggests a complex phase portrait for nonmonotone Biased Voter automata as the thresholds  $\theta_0, \theta_1$  vary, with solid growth for some choices, spreading rings in others, and mixed profiles for an intermediate regime. Indeed, some initial experimentation strongly suggests the existence of several phase transitions. Moreover, these systems are sufficiently simple, and closely related to Threshold Growth, that a rather complete understanding of their shape theory should be possible.

**Problem 4.** Let  $A_t$  be a Biased Voter automaton with range  $\rho$  box neighborhood, birth threshold  $\theta_0$  and survival threshold  $\theta_1$ . Assume that  $\theta_0 < \theta_1$  and  $\theta_0 \leq 2\rho^2 + \rho$ . Determine the dependence of the model's crystal growth on  $\rho, \theta_0, \theta_1$ , and the size and geometry of the initial seed  $A_0$ .

For the remainder of our study of deterministic growth we will restrict attention to totalistic Moore neighborhood models, focusing on the simplest nonlinear dynamics which exhibit complexity of various kinds. An especially fascinating class are the *Exactly  $\theta$*  solidification rules in which a vacant site becomes permanently occupied if exactly  $\theta$  of its 8 neighbors are occupied. Only the cases  $\theta = 1, 2, 3$  are capable of persistent growth from finite seeds, by comparison with  $\theta = 4$  Threshold Growth, which is convex-confined. Let us first consider the case  $\theta = 1$ .

### Exactly 1 Solidification

We will study the evolution starting from a single occupied cell at the origin in considerable detail. A key initial observation is that the locations  $(\pm t, \pm t)$  join the crystal at time  $t$ : the occupied set grows along the diagonals at the fastest possible speed,  $c = \sqrt{2}$ . This follows from the fact that, as in any Moore neighborhood CA started from  $\{0\}$ ,  $A_t \subset B_t = \{\|x\|_\infty \leq t\}$ , so by induction, at time  $t + 1$  each corner cell of  $B_{t+1} \setminus B_t$  sees only the diagonal cell that was added at time  $t$ . In general, by a *ladder* we mean any local CA configuration which propagates over time in some direction  $u$ , periodically in space. A *c-ladder* is a ladder which propagates with the fastest velocity allowed by  $\mathcal{N}$  (the “speed of light”). In the present case, the four diagonal trails are *c-ladders* one cell wide and with spatial period one. We will encounter more elaborate ladders later in the paper. For now, note that the Exactly 1 rule grows persistently from *any* finite  $A_0$  since there must be extremal occupied cells in the diagonal directions which give rise to permanent *c-ladders*.

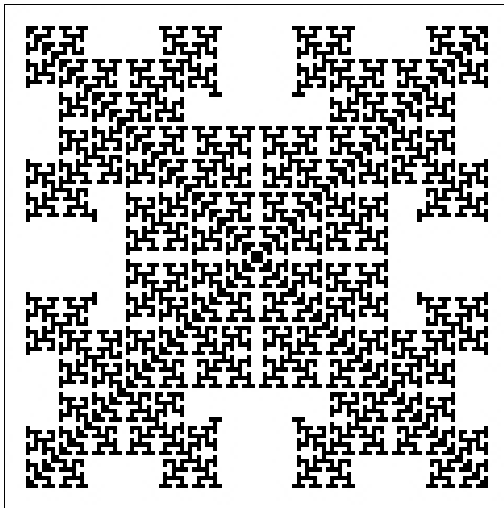


**Fig. 6.** The Exactly 1 Solidification Rule, started from a singleton, after 55 updates

Starting from  $\{0\}$ , the intricate growth of  $A_t$  off the diagonals is shown in Fig. 6 at  $t = 55$ . One immediately notices the recurring lace-like motifs, in striking contrast to any of the crystals discussed so far. More careful scrutiny reveals an exactly recursive structure along dyadic sequences  $t_n = 2^n$ , which

permits us to describe the occupied set at arbitrary times in terms of the binary expansion of  $t$ . This representation, in turn, lets us compute the asymptotic density with which the Exactly 1 rule fills  $\mathbb{Z}^2$ , subsequential limit shapes  $L_r$  along subsequences  $t_n = r2^n$ , and boundary lengths of the  $L_r$ . The same phenomenology is observed in many other intractable CA rules, so it is satisfying to quantify a “regular fractal pattern” [TM, p.39] which serves as an exactly solvable prototype for what Packard and Wolfram [PW] called growth with “corrugated boundaries.” Details follow.

Before proceeding, though, we pause to contrast the behavior of the most familiar and exactly solvable totalistic CA on  $B_1$  which generates a fractal: XOR over the Moore neighborhood. Starting from a singleton, that model generates a space-time pattern which is a slightly more complicated three-dimensional counterpart to the Sierpinski lattice obtained from Pascal's Triangle Modulo 2. In the same way that row  $2^n - 1$  of Pascal's Triangle has all odd coefficients and row  $2^n$  has only two, XOR on  $B_1$  fills each quadrant of  $B_{2^n}$  with a regular array of  $2 \times 2$  occupied boxes surrounded by empty frames of width 1 at time  $2^n - 1$ , and then collapses to only 9 occupied sites at time  $2^n$ . Evidently this process does *not* grow persistently, although it does have a disconnected limit shape  $L_r$  along each subsequence  $t_n = r2^n$  for fixed  $r \in (0, 1)$ . These shapes are cross-sections through a 3D fractal; almost all have density 0. See [Wil2] for an early account of the fractal structure of linear cellular automata. Linearity property (1.2 a) makes the analysis easy in comparison with Exactly 1, to which we now return.

### *The Exactly 1 recursion*

Let  $A_t$  be the occupied set at time  $t$  for the Exactly 1 rule started from  $A_0 = \{0\}$ . At times  $t_n = 2^n$ ,  $n \geq 3$ , we claim that the crystal has the following properties in the octant  $\{0 \leq x_2 \leq x_1\}$  (with analogous structure over the rest of the lattice, by symmetry):

(i) The only occupied site with  $x_1 \geq 2^n$  is  $(2^n, 2^n)$ . All other sites of the form  $(2^n, x_2)$  are vacant, with at least two occupied neighbors of the form  $(2^n - 1, y)$ , and so never join the crystal.

(ii) The only occupied site with  $x_2 = 0$  is the origin, and the occupied sites with  $x_2 = 1$  have first coordinates  $1, 3, 7, \dots, 2^n - 1$ .

(iii) The configuration on the lattice region bounded by  $(2^{n-1}, 2^{n-1})$ ,  $(2^n - 1, 2^{n-1})$ , and  $(2^n - 1, 2^n - 1)$  is an exact translate of the configuration on the region bounded by  $(0, 0)$ ,  $(2^{n-1} - 1, 0)$ , and  $(2^{n-1} - 1, 2^{n-1} - 1)$ . The configuration on the region bounded by  $(2^{n-1}, 2^{n-1})$ ,  $(2^n - 1, 2^{n-1})$ , and  $(2^n - 1, 1)$  is the mirror reflection of the same pattern. Finally, the configuration on the region bounded by  $(2^{n-1} + 1, 2)$ ,  $(2^n - 2, 2)$ , and  $(2^{n-1} + 1, 2^{n-1} - 1)$  is an exact rotated translate of the configuration on the region bounded by  $(2, 2)$ ,  $(2, 2^{n-1} - 1)$ , and  $(2^{n-1} - 1, 2^{n-1} - 1)$ , and all sites in lattice intervals  $\{2^{n-1}\} \times [2, 2^{n-1} - 1]$ ,  $[2^{n-1}, 2^n - 1] \times \{0\}$  and  $[2^{n-1}, 2^n - 2] \times \{1\}$  are vacant.

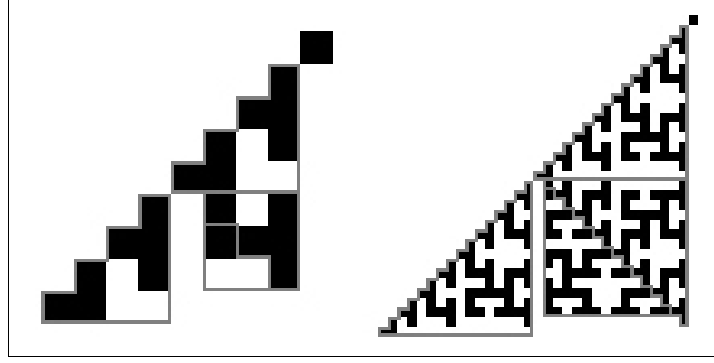


**Fig. 7.** One octant of Exactly 1 Solidification, started from a singleton, after 8 and 32 updates

Fig. 7 shows the configurations on the octant at time 8 ( $n = 3$ ) and time 32 ( $n = 5$ ). Properties (i)-(iii) may be verified at time 8 by inspection, and at subsequent times  $t_n = 2^n$  by induction. Assuming the hypothesis for  $n$ , the key observations are that  $c$ -ladders emanate from  $(2^n, 2^n)$ , one proceeding along the diagonal  $x_2 = x_1$ , and one heading “southeast” along  $x_2 = -x_1$ , and that by symmetry all sites of the form  $(x_1, 2^n)$  with  $2^n + 2 \leq x_2 \leq 2^{n+1} - 1$  are vacant (after time  $2^n + 1$  any such site which is unoccupied must have an even number of occupied neighbors, and so cannot join the crystal). Thus further growth within the octant is divided into three triangular regions, as in (iii) but with  $n$  replaced by  $n + 1$ , which evolve independently with mixed “all 1” and “all 0” boundary conditions. The first two new regions exactly replicate the conditions of the octant up to time  $2^n - 1$ , and so generate the same structure as claimed. The final triangular region also replicates this structure after a slight displacement. The  $c$ -ladder along its upper edge proceeds southeast until it occupies the point  $(2^{n+1} - 1, 1)$ , as desired in part (ii) of the induction. We omit further details, which are checked in a similar fashion.

### *Evaluation of the density*

Write  $a_n = |A_{2^n-1}|$ , and  $b_n = |A_{2^n-1} \cap \{x_1 \geq 0, 0 \leq x_2 \leq x_1\}|$ . Note first that, dividing the lattice into octants and appealing to symmetry,  $a_n = 8(b_n - 2^n - 1) + 4(2^n - 2) + 9$  for  $n \geq 1$ . Here the first term counts occupied sites not on the diagonals  $x_2 = \pm x_1$  and outside  $B_1$ , the second term counts occupied sites on the diagonals and outside  $B_1$ , and the third term counts occupied sites inside  $B_1$ . Thus,

$$a_n = 8b_n - 4 \cdot 2^n - 7.$$

Next, denote the triangular regions shown in (the right half of) Fig. 7, counterclockwise from the bottom left, by I, II, III, and IV. Then the four contributions to  $b_{n+1}$  have cardinality  $b_n$  (I and IV),  $b_n - 2$  (III), and  $b_n - (2^n - 2) - n - 2$  (II). For the last formula note that, as mentioned earlier, if one cuts from I the diagonal, and the sites with  $x_2 = 1$ , and the sites with  $x_2 = 0$ , then the remainder is isomorphic to II.

Therefore,

$$b_{n+1} = 4b_n - 2^n - n - 2,$$

and so

$$\begin{aligned} a_{n+1} &= 8(4b_n - 2^n - n - 2) - 4 \cdot 2^{n+1} - 7 \\ &= 4(8b_n - 4 \cdot 2^n - 7) + 16 \cdot 2^n + 28 - 8 \cdot 2^n - 8n - 16 - 4 \cdot 2^{n+1} - 7 \\ &= 4a_n - 8n + 5. \end{aligned}$$

The solution is

$$a_n = \frac{4^{n+2} + 24n - 7}{9}.$$

In particular we see that  $a_n/|B_{2^{n-1}}| \rightarrow \frac{4}{9}$ , the asymptotic density, and so  $2^{-n}A_{2^n} \rightarrow \frac{4}{9}1_L(x)dx$ , where  $L = \mathcal{B}_1 = \{\|x\|_\infty \leq 1\}$ , in the sense of (3.3).

Let us pause here to pose four problems. The first two are exercises for the enterprising reader. The third, motivated by empirical observation that many small seeds induce bounded perturbations of the singleton-seed recursion, may well involve substantial effort. The fourth is quite likely most difficult.

**Problem 5.** Packard and Wolfram [PW] observed similar behavior in the Exactly 1 rule on the nearest neighbor *diamond* (cf. rule 174, shown in their Fig. 2), although they did not identify a recursive structure or compute its asymptotic density. Mimic the derivation above to show that the density starting from a single occupied cell equals  $\frac{2}{3}$ .

**Problem 6.** Starting from a single occupied cell, compute the asymptotic density of the Exactly 1 Or At Least  $\theta$  solidification rule (in which  $\beta(i) = 1$  iff  $i = 1$  or  $i \geq \theta$ ) for  $2 \leq \theta \leq 8$ .

**Problem 7.** Does the Exactly 1 solidification rule on the Moore neighborhood fill the plane with asymptotic density  $\frac{4}{9}$  starting from *any* initial seed?

**Problem 8.** Find an elementary CA (solidification or otherwise) with a computable asymptotic density which is irrational.

### *Subsequential limit shapes*

Closer inspection of Exactly 1 recursive growth, driven by  $c$ -ladders, identifies asymptotic shapes  $L_r$  along all subsequences  $t_n = r2^n$  for fixed  $r$ . The limits are generated by a recursive scheme reminiscent of the von Koch algorithm [vK]. To describe it, introduce the binary expansion  $r = \sum_{k_0}^{\infty} d_k 2^{-k}$ ,  $k_0$  an integer, and  $d_{k_0} = 1$ . Write  $\mathcal{B}_s = \{x \in \mathbb{R}^2 : \|x\|_\infty \leq s\}$ . Starting from  $\mathcal{B}_{2^{-k_0}}$ , successively add three

translates of  $\mathcal{B}_{2^{-k}}$  for every  $k > k_0$  such that  $d_k=1$ , at the “exposed” corners of each previous square. Fig. 6 is suggestive of the algorithm for  $r = .111 = \frac{7}{8}$ . Note that smaller squares are added at each of four corners of the initial square, but only three of four corners are exposed at later stages.  $L_r$  is the monotone limit when this recursion is carried out for all  $k \geq k_0$ . Note that  $L_{2r} = 2L_r$ , so by normalizing suitably it suffices to consider  $r \in [\frac{1}{2}, 1)$ . Now the same methods as for the case  $r = 1$  can be used to show that  $\lim_{n \rightarrow \infty} t_n^{-1} A_{t_n} = \frac{4}{9} 1_{r^{-1}L_r}(x) dx$  in general. Thus we have our first example where (i) of (1.5) holds, but (ii) fails, with convergence to distinct limit shapes along suitable subsequences. All of these “corrugated” subsequential limits except  $L_1 = \mathcal{B}_1$  are nonconvex, and as we are about to see, many (e.g.,  $L_{\frac{6}{7}}$ ) have genuinely *fractal* edges, i.e., boundary curves with self-similar pieces of dimension greater than one.

### Asymptotic boundary length

Let us conclude our discussion of the Exactly 1 rule by analyzing the lengths of its asymptotic boundaries. First suppose  $r = \sum_1^N d_k 2^{-k} \in [\frac{1}{2}, 1)$ , with  $d_N = 1$ , and write  $\sigma_k = \sum_1^k d_l$ . Then it is not hard to check by induction that the boundary length  $\lambda(r)$  of  $L_r$  is given by

$$\lambda(r) = \frac{4}{3} \left[ 1 + \frac{4}{3} \sum_{k=1}^N d_k 3^{\sigma_k} 2^{-k} \right].$$

Hence, if  $r$  has a non-terminating binary expansion,

$$\lambda(r) = \frac{4}{3} \left[ 1 + \frac{4}{3} \sum_{k=1}^{\infty} d_k 3^{\sigma_k} 2^{-k} \right].$$

This asymptotic boundary length  $\lambda$ , as a function of  $r$ , is lower semicontinuous, sometimes finite and sometimes infinite, but not continuous at any value where it is finite. Assuming that  $\sigma_k/k \rightarrow \sigma$ , the Hausdorff dimension of the boundary of  $L_r$  is given by  $\max\{1, \sigma \frac{\ln 3}{\ln 2}\}$ . Thus, the Hausdorff dimension is not continuous anywhere: within any  $\epsilon$ -neighborhood of any  $r_0$  there is an  $L_{r_1}$  with boundary of finite length (dimension 1), an  $L_{r_2}$  with boundary of the largest possible dimension  $\frac{\ln 3}{\ln 2}$ , and a limit shape with any intermediate dimension as well.

## Exactly 2 Solidification

We conclude this section by turning to the Exactly  $\theta$  solidification rule with  $\theta = 2$ . How does a crystal grow from small seeds when exactly 2 of 8 neighbors must be occupied for a vacant site to join? Now a singleton obviously does nothing, but observe that a  $2 \times 2$  initial seed spreads in the shape of a diamond, with density  $\frac{3}{4}$  and speed 1 along the axes. (The computation is quite doable with paper and pencil.) Thus,  $t^{-1} A_t \rightarrow \frac{3}{4} 1_{\mathcal{D}}(x) dx$ , where  $\mathcal{D} = \{x \in \mathbb{R}^2 : \|x\|_1 \leq 1\}$ , in the sense of (3.3). The



evolution from this seed also reveals horizontal and vertical ladders of width 2 along the diagonals of the diamond which suggest a simple sufficient condition for growth in terms of an “exposed” dyad. Namely, suppose that, after suitable translation and reflection through one or both axes,  $A_0$  contains the dyad  $\{(0, 0), (0, 1)\}$  and is otherwise confined to the half-space  $\{x_1 < 0\}$ . Then, in the new coordinate system, a straightforward induction shows that  $A_t \supset \{0 \leq x_1 < t, x_2 = 0 \text{ or } 1\}$ . On the other hand, it is easy to check that no diamond seed  $D_n = \{x \in \mathbb{Z}^2 : \|x\|_1 \leq n\}$  grows at all, and that any  $n \times n$  square seed with  $n \geq 3$  stops after one step. Here we encounter our first growth model in which certain seeds grow, whereas others of arbitrarily large size do not, depending on the geometry. Is there any hope for a coherent shape theory in such a situation?

One approach, proposed by Packard and Wolfram [PW], is to study growth from *disorder*, e.g., from random subsets of a box  $B_L$ . Many CA rules exhibit a characteristic, linearly spreading shape when started from the vast majority of such random finite configurations. The Exactly 2 rule would seem to conform to this scenario, with limit  $\mathcal{D}$ , although the generic dynamics are sufficiently pseudo-random to offer little hope for rigorous results. A succession of horizontal and vertical ladders typically emerge from the edges of the crystal growth, the first such determining the extreme points of the limiting spreading diamond. Regions of regular growth with the pattern of the  $2 \times 2$  seed may also be observed. Indeed, even  $n \times 2$  rectangles for any  $n \neq 2$  exhibit essentially the same complexity as random seeds (apart from symmetry about the axes, of course). Fig.8 shows the evolution from a horizontal dyad at  $t = 100$ . Conceivably one could prove convergence to  $\mathcal{D}$  based on the regular emergence of indestructible ladders at the boundary, but the prospect seems too dim to pose this as an open problem.

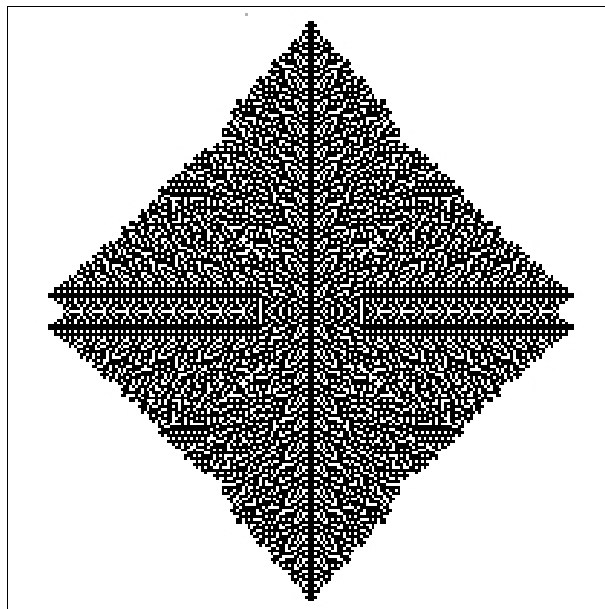


**Fig. 8.** Exactly 2 Solidification,  
from a horizontal dyad, after 100 updates

#### 4. Life without Death

The Exactly 3 growth model is one of our favorites — able to generate remarkably complex crystals, yet amenable to some substantive experimental mathematics. As noted in the Introduction, this is Conway's Game of Life with no  $1 \rightarrow 0$  transitions, so upon discovering its exotic properties a few years ago we named it *Life without Death* (LwoD, pronounced *el-wod*). Not surprisingly, we have since learned that some of the extraordinary behavior of this model has also been noted by Stephen Wolfram [Wol2] and various members of the *LifeList* Internet forum devoted to Conway's rule. The earliest reference to LwoD in the literature would appear to be [TM, pp.6-7].

Starting from most small seeds, e.g., from all lattice balls of “radius” up to 10, LwoD fixates. However, beginning with “radius” 11, as shown in Fig. 9 at time 1250, many such lattice balls produce spreading crystals reminiscent of the ancient Zia design on the New Mexico state flag. To highlight

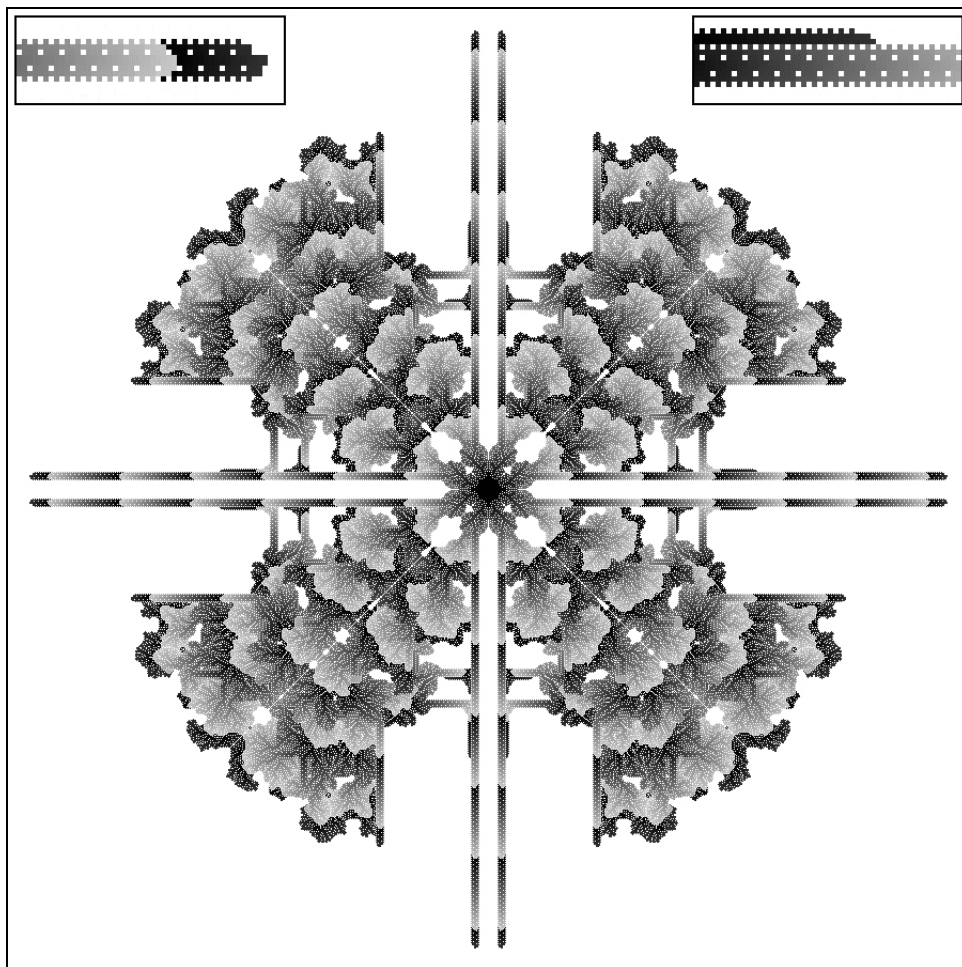


**Fig. 9.** Life without Death started from a lattice ball of “radius” 11. Insets at the upper left and right show a ladder tip, and parasitic shoot, respectively.

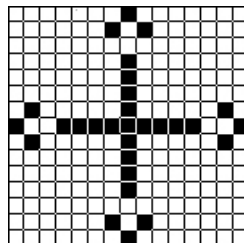
structural elements, we have drawn successive updates periodically using a 256-color gray scale gradient. Evidently, LwoD growth is dominated by a dendritic phase which we call *lava*, since its porous, seemingly organic form spreads slowly and unpredictably. Interspersed are horizontal and vertical *ladders* of a single design, which emerge seemingly at random from the lava, and advance at speed  $\frac{1}{3}$  by a back and forth weaving motion of period 12 with 4 spatial phases at the tip. The upper left inset of Fig. 9 magnifies one of the tips along the axes; of course the others are reflections and rotations by symmetry. Ladders seem to outrun the surrounding lava, suggesting that the recursive structures along the axes should persist indefinitely. But after more than 1100 updates, ladders which emerged from the lava collide with edges of the ladders along the axes, and parasitic *shoots* are formed. These structures, which can only evolve on the edges of ladders or other shoots, also emerge occasionally from the interstices between lava and ladders. Shoots have speed  $\frac{2}{3}$ ; one is magnified in the upper right inset of Fig. 9. Thus the parasites race along the edges of their host ladders until they reach the tips, at which time any of several lava eruptions takes place depending on the phase of the host-parasite interaction. Consequently, it is not at all clear whether LwoD started from the 11-ball grows persistently or fixates.

There are only two scenarios for which we know how to answer the persistence question. If the growth produces a fixed core surrounded by finitely many autonomous ladders extending away from the origin (with no active shoots!), then the growth persists, its asymptotic shape is the degenerate cruciform

$$C = \{|x_1| \leq \frac{1}{3}, x_2 = 0\} \cup \{x_1 = 0, |x_2| \leq \frac{1}{3}\},$$

and we obtain an example where (i) and (ii) of (1.5) hold, but (v) fails. On the other hand, if all shoots and ladders are stopped by interference with lava, and later the slow dendritic growth also grinds to a halt, then the system has fixated. Various small seeds lead to each of these outcomes, sometimes after hundreds or even thousands of updates. Empirical evidence, and a seeming affinity with stochastic dynamics, suggest *nucleation*: once a sufficiently large boundary layer of lava has formed, it would appear increasingly unlikely for all growth to stop. Here are two illustrative cases which can be resolved.

**Problem 9.** Run Life without Death for 100 updates starting from the 18-ball:  $\{\|x\|_2 < 18\frac{1}{2}\}$ , and for 1,000 updates starting from



to decide whether or not these processes grow persistently.

One can catalog all of the “elementary” interactions between pairs of ladders, and between shoots and ladders. For instance, synchronized ladders meeting at right angles can form a clean corner, ladders meeting head on can form a clean final border, and a ladder can be cleanly blocked by colliding at right angles with the side of another formed previously. Eruptions of lava, and shoot creation are also possible results, depending on the relative phases. It is less clear whether one can describe succinctly the preconditions for spontaneous emergence of shoots and ladders from lava. Regardless, the resulting complex dynamics self-organize so that very large motifs appear again and again as the crystal evolves. A striking example of this propensity, starting from an 80-ball, is discussed in an April 1995 recipe of [Gri2] (<http://www.math.wisc.edu/~griffeat/recipe26.html>). Over the first 10,000 updates a configuration of more than  $250 \times 250$  cells, containing an empty region larger than  $150 \times 150$ , replicates several times in the diagonal direction before being disrupted by a circuitous chain of interactions. Such complex manifestations invoke suspicions of even more exotic, unseen possibilities. Are there supremely powerful, but exceedingly rare, self-organizing LwoD structures? None has been observed from simple seeds or random initial conditions, but Noam Elkies (private communication) notes that there are  $c$ -ladder parasites capable of propagating between parallel sets of shoots on ladders.

In light of the previous paragraph, our favorite open question concerning LwoD is a difficult one.

**Problem 10.** Find a finite  $A_0$  from which LwoD grows persistently *and* fills  $\mathbb{Z}^2$  with positive density.

Experiments from large lattice balls suggest that such seeds abound. However, the only solution we can imagine would entail construction of a ladder gun, or some other space-filler analogous to those for Conway's Game which will be discussed in Section 6. We think there is at least a reasonable chance of such a recursive design, but its discovery would certainly require great ingenuity.

As an illustration that the complexity of LwoD can, to some extent, be characterized mathematically, we will now prove a result which captures its sensitive dependence on initial conditions.

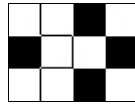
**Theorem 3.** Let  $A_t$  be Life without Death. Given any finite  $A_0$ , there are configurations  $C_1$  and  $C_2$ , each consisting of 28 cells, such that  $A_t$  grows persistently from  $A_0 \cup C_1$ , but fixates from  $A_0 \cup C_2$ .

(Note that the design and location of  $C_1$  and  $C_2$  are allowed to depend on  $A_0$ , but not their size.)

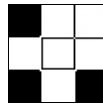
**Proof.** The idea is to form a closed frame around  $A_0$ , from a minimal number of strategically placed occupied cells, so that the growth emanating from  $A_0$  is completely confined by the time it reaches the frame. If the frame is static, then this should constrain growth to its bounded interior, thereby ensuring fixation. If the frame instead produces isolated ladders traveling away from its exterior, then since the growth of  $A_0$  is still controlled, persistent growth is guaranteed. Clearly, a closed  $\ell_1$ -circuit of occupied

sites (i.e., a loop of sites connected by  $N$ ,  $S$ ,  $E$ , and  $W$  transitions) prevents any interaction between the dynamics on its interior and those on its exterior. So our frame need only include such a circuit to achieve the desired containment.

The details of the construction are as follows. First, choose  $L$  so that  $A_0 \subset B_L$ . Next, for a suitably large  $N$ , place a 4-cell *side seed*



along the positive  $x_1$  axis so that the empty site between its top and bottom cells is located at  $(4NL + 1, 0)$ , and a 3-cell *corner seed*



in the first quadrant so that its middle cell is located at  $(4NL - 18, 4NL - 18)$ . Place 3 more such side seeds symmetrically along the axes (with their isolated cells closest to the origin), and 3 more corner seeds symmetrically along the diagonals of the other quadrants (with their middle cells closest to the origin). The 28-cell collection of corner and side seeds constitutes configuration  $C_1$  in the statement of the theorem. Configuration  $C_2$  agrees with  $C_1$ , except that

- the empty site between the top and bottom cells of the side seed along the positive  $x$ -axis is at  $(4NL, 0)$ ;
- the leftmost cell of this side seed is moved 9 sites further to the left (so that there are a total of 11 empty sites between it and the rightmost cell);
- the middle cell of the corner seed in the first quadrant is at  $(4NL - 22, 4NL - 22)$ ;

with symmetric changes to the other 6 seeds.

Easiest to check is the evolution of the side seed pictured above. With a little care and patience, one can verify by hand that the result is two ladders, traveling north and south, cleanly fused along the axis. Thus, the side seeds of  $C_1$  spread away from the axes to begin forming a frame. Simultaneously, as can only readily be checked with a computer, after a substantial but finite eruption of lava, the corner seeds each produce a pair of ladders heading from the diagonals toward the axes. The corner motifs of Fig. 10 illustrate this effect. Moreover, the offsets of +1 and -18 from  $4NL$  in our design ensure that the pairs of ladders heading toward one another are aligned exactly, and their collisions produce a clean closed frame with no additional shoots or lava. Since, as previously noted, the spatial phase of LwoD ladders is 4, that factor in our design ensures the same outcome, independently of  $L$  and  $N$ .

Configuration  $C_2$  evolves similarly, except that the side seeds produce two parallel ladders outside the frame traveling away from the origin, a substantial but finite lava eruption occurs inside the frame, and the ladders heading from the axes to the diagonals are displaced a few cells from their counterparts in  $C_1$ . In this case the corresponding offsets of 0 and -22 ensure a clean closed frame. Fig. 10 shows LwoD started from  $B_{15} \cup C_2$  after 350 updates in the case  $L = 15$ ,  $N = 3$ . By inspection, one easily finds a closed  $\ell_1$ -circuit embedded within the frame.

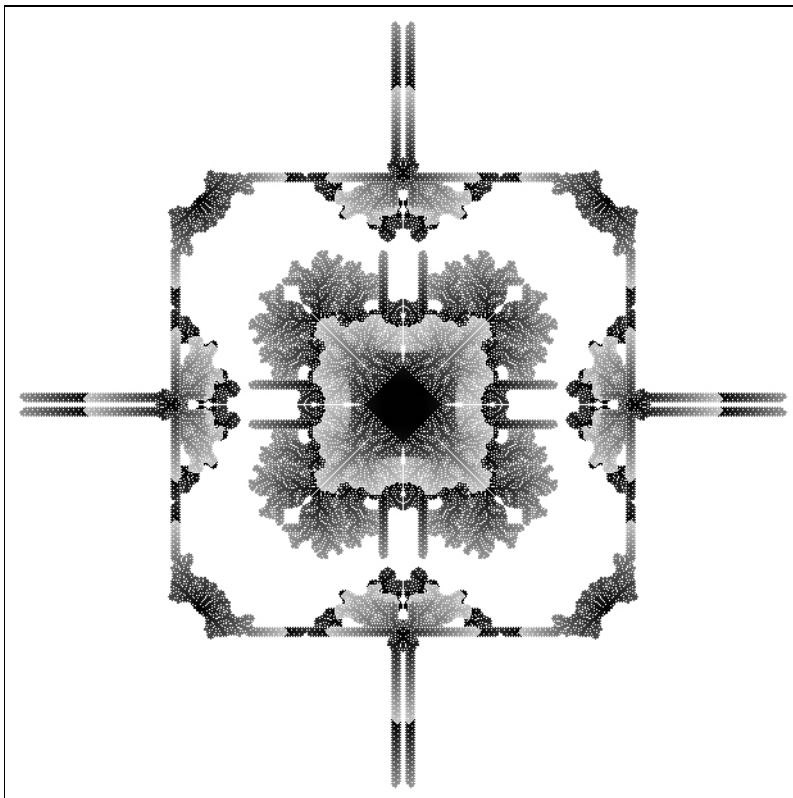


**Fig. 10.** Formation of a frame with exterior ladders from 28 cells.  
Here  $L = 15$ ,  $N = 3$ ,  $t = 350$ .

To complete the proof, it suffices to argue that for any  $L$ , and  $N$  sufficiently large, these constructions produce a complete frame before the growth from  $A_0$  can possibly interact with it. We show this by comparison with our Basic Example. If  $A_t$  denotes LwoD, and  $\bar{A}_t$  Threshold 3 Growth, both started from the same  $A_0$ , then it is easy to check recursively that  $A_t \subset \bar{A}_t$  for all  $t$ . Since LwoD ladders travel at speed  $\frac{1}{3}$ , and all lava eruptions within the frames are finite, both types of frame are complete by time  $6NL + c_1$ , for some constant  $c_1$ . Recalling from Section 2 that the asymptotic shape  $\mathcal{O}$  of our Basic Example has vertices  $(\pm \frac{1}{2}, 0)$ ,  $(0, \pm \frac{1}{2})$ , and  $(\pm \frac{1}{3}, \pm \frac{1}{3})$ , it follows that  $A_0 \subset B_L$  cannot possibly reach any site of either surrounding frame before time  $8NL - c_2$  for a constant  $c_2$  depending only on  $L$ . By that time, for  $N$  large, the frame is in place.  $\square$

**Problem 11.** Consider the threshold 2 forest fire  $\xi_t$ , a 3-state CA in which 0 (flammable) changes to 1 (burning) next time if 2 or more of the 8 nearest neighbors are currently burning, 1 updates to 2 (burnt) automatically, and 2's never change. Check that  $\xi_t$  supports width 2 ladder-like fire fronts, and then mimic the proof of Theorem 3 to show that persistence of fire (1's) depends sensitively on the initial configuration  $\xi_0$ .

As another indication of Life without Death's remarkable complexity, it is shown in [GM] that this rule can emulate any logical circuit. The ability to do so establishes a degree of algorithmic complexity known as *P-completeness* [GHR]. Simple CA models of ballistic computation are known to have this property; see Chapter 18 of [TM] for a nice exposition. The challenge with LwoD is to demonstrate how ladders, which leave tracks that cannot be crossed, nevertheless are able to compute starting from suitably designed initial conditions. Initially, the presence or absence of input ladders corresponds to whether or not respective logical inputs are true or false. One then designs interactions corresponding to AND, OR, NOT, and so forth, the truth of the circuit being determined by the presence of an output ladder. More generally, if a cellular automaton in two or more dimensions supports growing ladders which can turn, and can block each other, then it turns out that the dynamics can express arbitrary Boolean circuits. Fig. 11 shows a ladder interaction with 4 cells that leads to an especially graceful right turn. The ability of one ladder to block another at right angles was mentioned previously. As in the proof of Theorem 3, some rather delicate engineering is needed to control the model's propensity for parasitic shoots and chaotic lava; see [GM] for details. Once P-completeness is established, there is an illuminating corollary

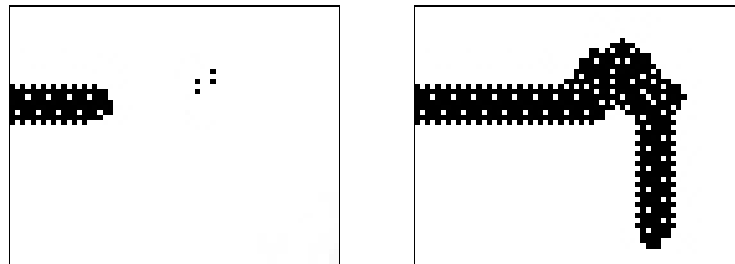


**Fig. 11.** Right turn of an LwoD ladder after collision with a 4-cell configuration

for growth theory. Namely, suppose we want to know whether a finite seed will grow persistently. If we design the seed so that only the corresponding circuit's output ladder can persist, then the CA will grow to infinity if and only if its circuit's output is true. Thus, growth model prediction is at least as hard as Boolean circuit prediction.

A number of minor variants of Life without Death admit ladders with similar architectures. Four totalistic alternatives we know have the same birth rule, but preclude survival for certain population counts: (a) 8, (b) 7, (c) 7 or 8, and (d) 1 or 3. The 2 OR 5 solidification rule of the next section supports

diagonal ladders, while the range 2 CA described in an August 1996 recipe of [Gri2] (<http://psoup.math.wisc.edu/recipe80.html>) has horizontal, vertical and diagonal ladders. Of course, these differences destabilize many, if not all, of LwoD's elementary interactions, so we invite the reader to investigate how many of the observations of this section carry over.

## 5. $\theta$ OR $\theta'$ Rules

Let us look next at slightly more complicated totalistic rules which seem to interpolate between Threshold Growth and the random systems to be discussed in the final section of this paper. Namely, we consider solidification dynamics with  $\beta = 1_{\{\theta, \theta'\}}$  ( $\theta < \theta'$ ). In words, a vacant site becomes occupied when it sees either  $\theta$  or  $\theta'$  occupied Moore neighbors, while occupied sites remain so forever. We will briefly describe some interesting examples with  $\theta = 2, 3$ .

Turning first to 3 OR  $\theta'$  rules, we note that for  $\theta' = 4$ , the process started from a range 1 diamond agrees *exactly* with Threshold 3 Growth as prescribed by (2.3) (cf. Fig. 1), so the limit shape is the same octagon  $\mathcal{O}$ . It is easy to check that  $\mathcal{O}$  is also the limit starting from any  $m \times n$  lattice rectangle of size at least 3. Of course 3 OR 4 will not completely fill the lattice from large  $A_0$  in general, since tiny holes such as single 0's completely surrounded by 1's cannot fill in. Roughly speaking, though, 0's along the exterior boundary of the crystal see at most four 1's, so this is a minor perturbation of the monotone case. Making the last observation precise is surprisingly difficult, since (1.3) is not available – try to find an airtight solution to our next problem.

**Problem 12.** Show that 3 OR 4 solidification, started from any finite  $A_0$  with persistent growth, covers a cofinite subset of the lattice with asymptotic shape  $\mathcal{O}$ .

At the other extreme, 3 OR 8 is an inconsequential perturbation of LwoD. One simply fills in the isolated vacant cells, by which we mean the exact connection described in the following puzzle.

**Problem 13.** Show that 3 OR 8 solidification, started from any finite  $A_0$  and run for  $t$  time steps, agrees with Life without Death run for  $t - 1$  time steps starting from  $A_0$ , followed by one final 3 OR 8 update.

More interesting (and much less tractable!) are the 3 OR  $\theta'$  rules with  $\theta' = 5, 6, 7$ . In each of these cases we start from a lattice ball of “radius” 10, and let the occupied region grow until it reaches the edge of an  $800 \times 800$  array, in order to get an initial impression of the purported limiting shape. To enhance visualization, each successive update is displayed in a new color from a gray scale palette. The results are shown in Fig. 12. Note that the boundaries of all three crystals exhibit pseudo-random



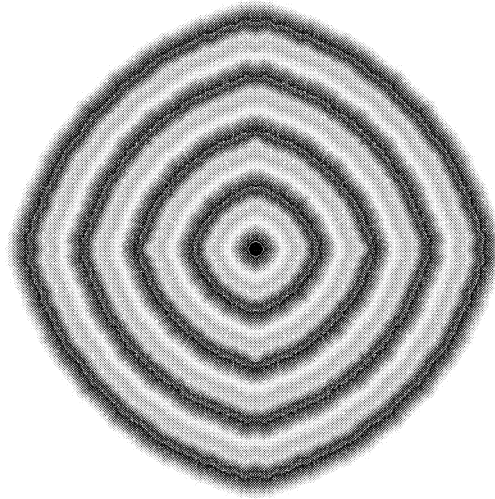


**Fig. 12a.** 3 OR 5 Solidification

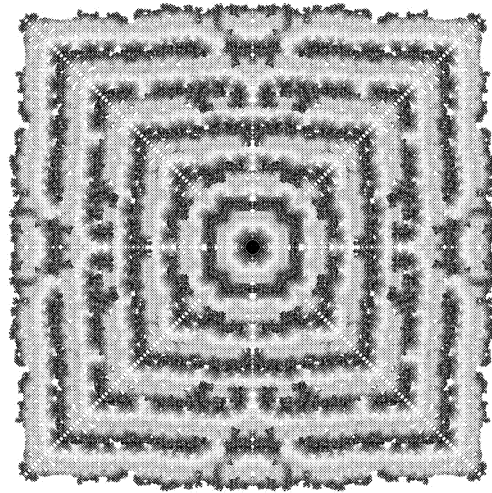


**Fig. 12b.** 3 OR 6 Solidification

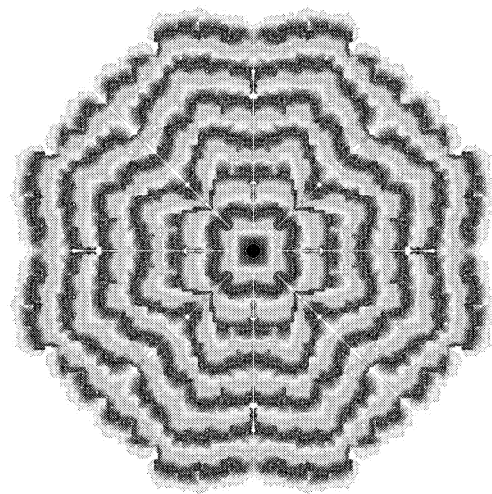


**Fig. 12c.** 3 OR 7 Solidification

fluctuations. The ability of simple CA dynamics to emulate stochastic interfaces was first observed by Vichniac [Vic], who introduced nonmonotone “twists” into systems such as Majority Vote.  $3 \text{ OR } 5$  is similar in spirit; Fig. 12a raises at least the prospect of a strictly convex limit shape with piecewise smooth boundary. Such shapes  $L$  are believed to arise from some of the simplest random growth models, as we will explain in Section 7. On the other hand, Figs. 12b and 12c suggest limit shapes of a square and octagon, respectively.

Precise analysis of any of these models seems prohibitive, so we resort to larger experiments on dedicated devices such as the CAM-8 [Marg] for further insight. This cellular automaton machine from the MIT Laboratory for Computer Science is a state-of-the-art of interactive desktop parallel processor, offering a unique combination of computing power and visualization capability for the study of CA dynamics. To date, our most interesting CAM-8 discovery about  $3 \text{ OR } 6$  growth is the emergence of certain structures, at the corners, with very large but finite period. Perhaps these can be used to confirm a square limit  $L$ , at least from some initial  $A_0$ . The  $3 \text{ OR } 7$  growth rule is illuminating for a couple of reasons. First, CAM-8 experiments on larger arrays indicate rather convincingly that its limit shape  $L$  is *not* an octagon as one might surmise from Fig 12c, but rather a shape with piecewise smooth boundary more like the one suggested by Fig 12a. Polygonal corners would seem to be a short-term artifact of close-to-critical dendritic growth. In addition, Dean Hickerson (private communication) has recently discovered that  $3 \text{ OR } 7$  grows *sublinearly* from certain seeds, our first bona fide counterexample to (1.5i).

**Problem 14.** Check that  $3 \text{ OR } 7$  is persistent and sublinear when started from the 3-ball  $\{\|x\|_2 < 3\frac{1}{2}\}$  by showing that  $t^{-\frac{1}{2}}A_t \rightarrow \{\|x\|_\infty \leq 2\sqrt{\frac{2}{3}}\}$  as  $t \rightarrow \infty$ .

In light of the complicated scenarios described in the previous paragraph, it is rather surprising that the  $2 \text{ OR } 5$  rule produces an assortment of recursive crystals, thereby providing our first example of a CA for which different seeds are known to yield different nontrivial asymptotic shapes. Moreover, some are convex, some not. We will exhibit growth crystals starting from  $r$ -balls  $\{\|x\|_2 < r + \frac{1}{2}\}$  for several values of  $r$ . The exact evolution of each can be confirmed using formalism (3.1). First, when  $r = 2$  (a  $5 \times 5$  box with the 4 corner sites removed), a convex octagon with sides of slope  $\pm 3$ ,  $\pm \frac{1}{3}$  emerges, as shown in Fig. 13. The same limit occurs from  $r = 3$ . But starting with  $r = 4$ , nonconvex shapes arise.

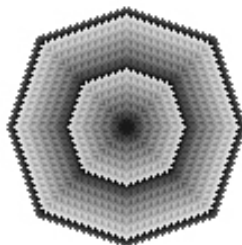


Fig. 13.  $2 \text{ OR } 5$  Solidification from a small seed

(A curious exception is the  $r = 8$  case, which stops growing after a single update.) Some of these elegant crystals, corresponding to  $r = 9, 12$  and  $13$ , are shown in Fig. 14. Note the fixed-width indentations and diagonal ladders of the first two rules, which do not figure into the limit since they are negligible after normalization. In the first two cases, then,  $L$  is the same nonconvex octagon, with slopes  $\pm \frac{1}{2}, \pm 2$ . The

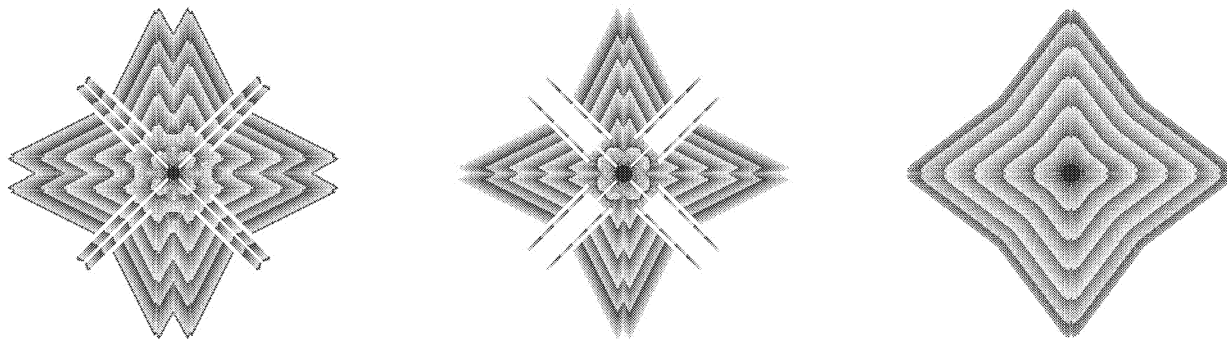


Fig. 14: 2 OR 5 Solidification from lattice balls of “radius” 9, 12, and 13, respectively

last case yields a different nonconvex octagonal limit with slopes  $\pm \frac{3}{4}, \pm \frac{4}{3}$ . Thus (i), (ii) and (v) of Theorem 1 seem to hold, but (iii) and (iv) fail, for this growth model. To conclude this section, we offer two instructive exercises. The first is easy to do with paper and pencil, whereas the second can only be solved using *WinCA* or some other CA experimentation platform capable of handling large arrays.

**Problem 15.** Show that 2 OR 5 solidification starting from a horizontal dyad grows at distinct speeds in the horizontal and vertical directions, thereby providing our first example of a two-dimensional limit shape which is not balanced with respect to the origin. Compute the asymptotic shape  $L$ .

**Problem 16.** Show that the asymptotic shape  $L$  of 2 OR 5 solidification is the same starting from the 14-ball  $A_0 = \{\|x\|_2 < 14\frac{1}{2}\}$  as from the 9- or 12-ball.

## 6. Exotic Case Studies

Growth generated by maps  $\mathcal{T}$  which are neither monotone nor solidification rules often displays bewildering complexity. This section describes three totalistic models with particularly intriguing dynamics, largely beyond the reach of mathematical understanding, but raising many fundamental questions about the scope of possible behaviors for the simplest cellular automata.

## Wolfram's Crystal

Can the asymptotic shape  $L$  for a simple CA growth rule be a perfect Euclidean circle? As mentioned at the beginning of this survey, Packard and Wolfram seemed to indicate “yes” in their seminal 1985 paper [PW], both in the passage cited in our Introduction, and later when they summarize:

*“A remarkable feature [of diffusive CA growth] is that the boundaries of the patterns produced do not follow the polytopic form suggested by the underlying lattice construction of the cellular automaton. Indeed, in many cases, asymptotically circular patterns appear to be produced.”*

The authors cite a few examples of “diffusive growth,” by which they apparently mean slow linear growth; just how slow is unclear. For instance, they include pictures of the perturbation of Conway's Life with  $\beta = 1_{\{3\}}$  and  $\sigma = 1_{\{2,3,4\}}$  up to about time 100 starting from a small irregular seed. Their final configuration is still quite irregular, but vaguely circular.

The *isotropy problem* for spatial growth – whether local interacting dynamics can give rise to an asymptotic shape which is radially symmetric – dates back forty years to Eden's Model [Ede], in which a new cell is repeatedly added at a random boundary location of the crystal. For many years it was conjectured that  $L$  for that model should be isotropic. Although the two and three dimensional cases remain open, more recent supercomputer simulations, and rigorous counterexamples in high dimensions [Kes2], provide rather convincing evidence of a residual lattice effect in the limiting geometry of Eden's Model. We will briefly discuss other shape results for random growth in the next section.

For deterministic CA dynamics, an analysis in [GG1] shows that Threshold Growth with moderate range  $\rho$  and suitably chosen threshold  $\theta$  can achieve a polygonal asymptotic shape which approximates a circle within 2%. We also saw suggestive evidence in the last section that  $L$  for the 3OR5 rule may be anisotropic with smooth boundary segments. Evidently, then, we are dealing with a very subtle question here, which cannot be resolved by cursory inspection of a few small computer experiments.

About two years ago we met with Wolfram [Wol2] to discuss the isotropy problem. He confided that, upon closer inspection, the examples mentioned in [PW] did *not* appear to grow with radial symmetry. But he described an exhaustive search of all totalistic CA, and mentioned another rule which seemed to do the best job of growing circles. *Wolfram's Crystal* is another perturbation of Life, with  $\beta = 1_{\{3\}}$  and  $\sigma = 1_{\{0,1,2,3,4\}}$ . Fig.15 shows its evolution from a 10-ball after 1,000 updates. This preliminary picture was sufficiently tantalizing that we designed a much larger experiment using our CAM-8 “mixmaster.” To test the isotropy conjecture, we captured Wolfram's Crystal every 500 updates until it filled an 8K  $\times$  8K array. As a test for circular  $L$ , we measured the extent of the growth in the horizontal and 45° directions at times 500, 1000, ..., 10000 (starting from a somewhat larger lattice

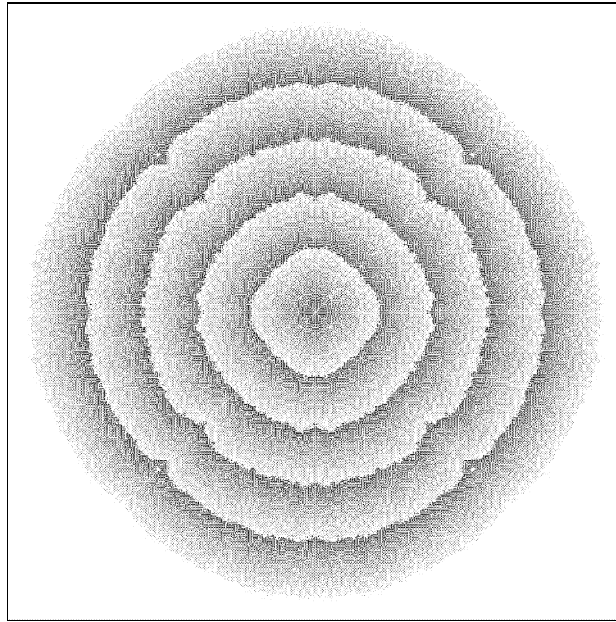


**Fig. 15.** Wolfram's Crystal from a 10-ball at time 1,000

circle). More precisely, at each such time we computed the distance from the origin to the closest hyperplanes touching the occupied set, and normal to the  $0^\circ$  and  $45^\circ$  directions. The results  $h_t$  and  $d_t$ , together with the eccentricity  $e_t := h_t / \sqrt{2} d_t$ , are tabulated in the Table below. We leave it to the reader to decide whether the numbers support isotropy, or whether there is a residual eccentricity on the order of

| Time $t$ | Horizontal Displacement $h_t$ | Diagonal Displacement $d_t$ | Eccentricity $e_t$ |
|----------|-------------------------------|-----------------------------|--------------------|
| 500      | 269                           | 180.5                       | 1.054              |
| 1000     | 453                           | 307                         | 1.043              |
| 1500     | 643                           | 432                         | 1.052              |
| 2000     | 823                           | 559.5                       | 1.040              |
| 2500     | 1005                          | 685.5                       | 1.036              |
| 3000     | 1192                          | 810.5                       | 1.040              |
| 3500     | 1368                          | 934.5                       | 1.035              |
| 4000     | 1556                          | 1056                        | 1.042              |
| 4500     | 1746                          | 1183.5                      | 1.043              |
| 5000     | 1931                          | 1310.5                      | 1.042              |
| 5500     | 2110                          | 1436                        | 1.039              |
| 6000     | 2296                          | 1563.5                      | 1.038              |
| 6500     | 2481                          | 1686                        | 1.041              |
| 7000     | 2669                          | 1816.5                      | 1.039              |
| 7500     | 2854                          | 1941.5                      | 1.039              |
| 8000     | 3037                          | 2065.5                      | 1.040              |
| 8500     | 3217                          | 2190.5                      | 1.038              |
| 9000     | 3399                          | 2317.5                      | 1.037              |
| 9500     | 3582                          | 2443                        | 1.037              |
| 10000    | 3768                          | 2569.5                      | 1.037              |

**Table.** Horizontal and Vertical Extent of Wolfram's Crystal up to time 10,000

a few per cent. Regardless of the interpretation, a rigorous mathematical solution to either part of our next problem would constitute a major milestone in the theory of cellular automata shapes.

**Problem 17.** Find a CA (with  $\mathcal{N}=B_\rho$  for some  $\rho$ , say) having an asymptotic shape  $L$  which is two-dimensional and convex, but not a polygon. Is there such an example for which  $L$  is a circle?

### Hickerson's Diamoeba

As non-monotone cellular automata go, Wolfram's crystal is quite well-behaved. Despite its complicated boundary dynamics, the growth spreads steadily – albeit slowly – and appears to acquire a characteristic shape. By way of contrast, we now introduce an incredibly wild totalistic CA discovered by Dean Hickerson, and called the *Diamoeba* for reasons that will become clear shortly. Its birth and survival maps are

$$\beta = 1_{\{3,5,6,7,8\}} \text{ and } \sigma = 1_{\{5,6,7,8\}}.$$

Note that this rule is interfacial. Nevertheless, its evolution from simple seeds is so complex that we still do not know, or even hazard to guess, whether persistent growth is possible. We extend our gratitude to Hickerson for letting us describe his findings, some of which have been posted to the (private) *LifeList* Internet discussion group, but are otherwise unpublished.

From small random seeds the Diamoeba typically dies out, although a few configurations have period 2. For instance, the lattice box with 4 cells on a side is such a “blinker.” Larger squares with even side length  $2n$  grow to diamonds of twice the size, but then lock into a period 2 orbit, as we invite the reader to verify.

**Problem 18.** Carefully describe the asymptotic behavior of Diamoeba from lattice boxes with an *even* number of cells on a side.

Much more interesting is the fate of square seeds  $B_n$ , with odd side length  $2n+1$ . Early in our experimentation with Hickerson's Diamoeba, we noticed that these initial configurations first grow into (near-) diamonds, as in the case of even side length, but then begin a complicated withering process until they vanish completely ! For instance, Fig. 16 shows the collapse after  $B_{150}$  has spread to a 300-diamond, with level sets of the shrinking boundary drawn using a periodic gray scale palette. We observed the cyclic occurrence of several distinct polygonal shapes, and suggested to Hickerson that the evolution appears recursive. Not only did he confirm our conjecture, but he was also able to obtain an exact expression for the lifetime of the process as a function of  $n$ .

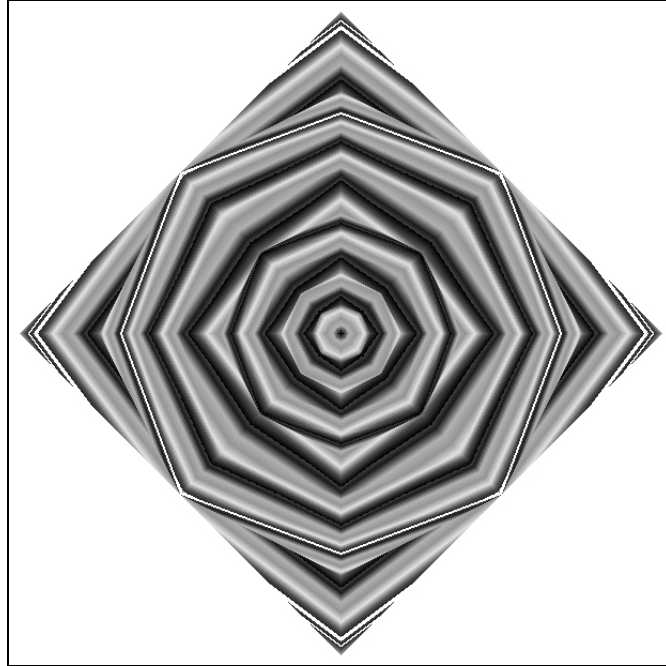


**Fig. 16.** Oscillating collapse from  $B_{150}$

During the first  $n$  updates the shape is a 12-gon which interpolates between the original square and the maximal diamond. From time  $n$  to  $2n$  the shape is a shrinking 12-gon. After that, most shapes in the collapse are 16-gons, some convex, some not, which interpolate between a cycle of 6 characteristic octagons with slopes  $\frac{3}{4}, \frac{1}{2}, \frac{3}{8}, \frac{11}{24}, \frac{1}{2}$  and  $\frac{2}{3}$ , respectively (along with their negatives, reciprocals, and negative reciprocals). Summation of an infinite geometric series shows that the time  $\tau_n$  until death is asymptotic to  $12n$ , while Hickerson's detailed analysis yields the exact formula

$$\tau_n = 12n - 8 - 4n_1 + 2n_{11} + (n \bmod 2).$$

Here  $n_1$  and  $n_{11}$  are the number of 1's and the number of adjacent 11 pairs in the binary representation of  $n$ . (For instance,  $\tau_{150} = 12 \cdot 150 - 8 - 4 \cdot 4 + 2 \cdot 1 + 0 = 1778$ , as is readily confirmed by experiment.) We remark that other large, lattice-symmetric seeds such as lattice  $r$ -balls are drawn toward this collapsing attractor.

In light of the discussion so far, one might be tempted to conclude that the Diamoeba either fixates or dies out, possibly after a modest growth spurt, from any initial seed. However, even moderately large initial configurations with slight lattice asymmetry can tell a very different story. As an illustration, let us consider seeds of size  $2N - 1$ : rectangles 2 cells high and  $N$  cells wide, but with the upper right corner cell removed. The cases  $N \leq 64$  all die by time 10,000, except for  $N = 34$  and 43, which stabilize as period 2 blinkers within a few thousand generations, and the four cases  $N = 54, 59, 61, 63$  whose behavior we will now describe in some detail.

The *Diamoeba* first truly lives up to its name when  $N = 54$  or  $59$ . If  $N = 54$ , then after rapidly forming a rough diamond within the first 25 updates, asymmetry at the boundary leads to chaotic time intervals of growth and collapse. Occasional interfacial “shocks” cause size fluctuations on the order of the entire crystal. In real time, the growth seems almost organic, like the undulations of a single-celled creature. This effect is heightened by the dynamics of virtual *cilia* which run along *Diamoeba*'s boundary (cf. the upper left inset of Fig. 17, for the case  $N = 59$ ). The net effect after 50,000 updates is a blob of more than 50,000 cells, suggesting omnivorous growth (with a modest appetite). However, at generation 52,150 the process seems to stop growing, at least for a very long while. Its shape is roughly an oblong diamond, a recurring geometry for *Diamoeba*, while its population fluctuates only a few hundred cells away from 67,500. Examination of the cilia along the edges explains this hiatus. The northwest edge is period 2, except for a small period 8 region at its top. The top half of the northeast edge and about the bottom  $\frac{1}{3}$  of the southeast edge also have period 2. Three independent boundary regions are still active: the lower half of the northeast edge, the upper  $\frac{2}{3}$  of the southeast edge, and the entire southwest edge. Further computation shows that the northeast region becomes period 4,088 in generation 952,824 and the southeast region becomes period 167,409,998 in generation 731,625,667. Alas, Hickerson has checked that the longest, southwest region remains aperiodic for more than 200 billion updates without experiencing a shock that destabilizes its shape and starts another growth spurt. The eventual fate of this process remains unresolved. If tempted to conclude that the crystal has stopped growing, you might ask yourself why. A  $3 \times 199$  rectangular seed is instructive in this regard: within about 2,500 updates it stabilizes as a ciliated diamond of approximately 13,000 cells, retains essentially the same formation until shortly after time 99,000, but then starts changing shape again..

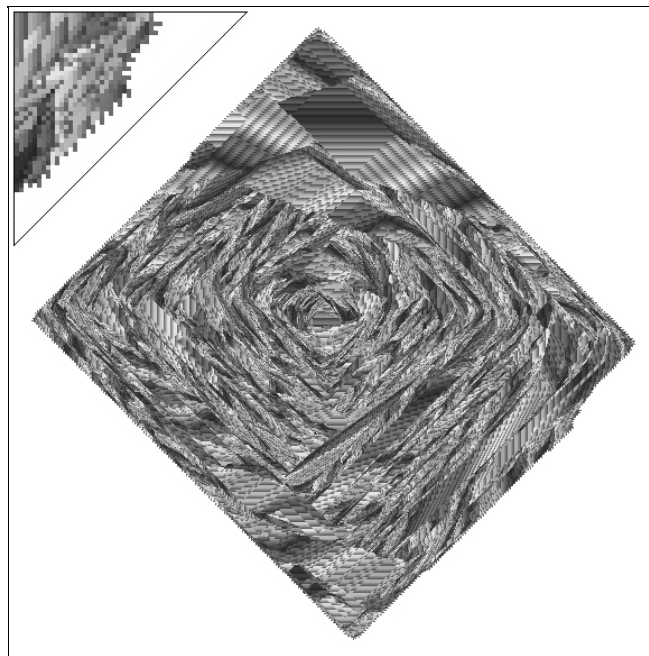


**Fig. 17.** Chaotic growth of Hickerson's *Diamoeba* from a  $2 \times 59$  rectangle with one cell removed



The case  $N = 59$  is a better candidate for persistent growth, but ends up creating even more confusion. Fig. 17 shows its growth during the first 50,000 updates using a cyclic gray scale palette to represent cells added at successive times. The intricate fossil-like striations reflect the chaotic ebb and flow of Diamoeba growth. A detail at the upper left shows cilia below the right corner. After about 940,000 updates the crystal stops growing temporarily, with a population of around 41,900,000 cells. Hickerson has actually identified 6 different patterns of cilia which arise along the edges of Diamoeba and can be modeled exactly by one-dimensional CA rules with boundary conditions. For instance the linear XOR rule arises frequently. By isolating the boundary dynamics and feeding them to a 1D simulator he is able to predict that one of the cilia regimes will break down after another 5,191,475 updates, after which another growth spurt is possible. He speculates that alternating cycles of growth and stasis arise as the different 1D CA rules compete for supremacy along the boundary, but that eventually a single rule should attain dominance along each edge of the rough diamond, and then, perhaps eons later, the Diamoeba should finally settle into a periodic state.

Growth stops for  $N = 61$  around generation 109,000 with a population of about a quarter of a million cells. The  $N = 63$  case is settled by time 14,276, with an  $86 \times 86$  bounding box and periodic 1D CA dynamics along the four sides of its diamond. The periods of these rules – 1478, 1246, 2936, and 4628 – are small enough that the period of the entire crystal is computable as 17,572,432,696.

For values of  $N$  above about 65, there seems to be a kind of nucleation transition: the great majority of seeds grow to at least a very large size. Over the range  $[65, 85]$ , only the cases 69 and 73 die out within the first 100,000 updates, none of the others become period 2 within that time span, only 77, 80 and 83 *appear* to have stopped (like 54), and the remaining 16 cases seem to still be growing, with bounding boxes between about 500 and 1000 cells on a side. Now that our readers are completely bewildered, we finish this subsection with an open problem which can perhaps be resolved by very clever construction of a seed that grows recursively.

**Problem 19.** Does Hickerson's Diamoeba fill  $\mathbb{Z}^2$  starting from some initial seed  $A_0$  ?

## Conway's Life

John Conway's Game of Life, the totalistic rule with birth and survival maps

$$\beta = 1_{\{3\}} \text{ and } \sigma = 1_{\{2,3\}}$$

is without question the most celebrated of all cellular automata. Popularized by Martin Gardner in a series of Scientific American articles [Gar1] beginning in 1970, the model rapidly became a favorite

experimental playground of recreational mathematics. For a superb account of the early years, see volume 2 of [BCG]. More recently, Conway's Game has been recognized as one of the first and simplest prototypes for the emerging arena of complex systems theory known as Artificial Life (cf. [Lan]). Perhaps surprisingly, despite the intense scrutiny this rule has received for nearly 30 years, exciting new discoveries continue to be made, while many fundamental questions remain unresolved. We are by no means experts, but will attempt to summarize here some recent developments relating to persistent growth from finite seeds. For clarity, the discussion is divided into three subsections.

### *Universality and Pattern Synthesis*

One of Life's most famous properties is *computation universality*, a stronger form of the circuit emulation for Life without Death which was described in Section 4. The counterparts of LwoD's ladders are moving *gliders*, various *eaters* which can block gliders without being damaged, and *glider guns* such as the famous 45-cell construct for which Bill Gosper won a \$50 prize from Conway. Life does not share LwoD's propensity for unbridled chaotic growth, so using these ingredients identified in the early 70s, one can simulate a Turing machine with its infinite storage capacity. Consult [BCG] for details, and [Min] for theoretical background. Refinements by Hickerson and Callahan (cf. [Cal]) have simplified the construction and improved its theoretical efficiency.

Life experts vouch for the feasibility of a much more powerful (and complicated) extension of the Turing scheme which establishes *construction universality*, meaning that Life can faithfully simulate *any* CA rule in space. Although details of the general construction have never been specified, at least in principle Life could then grow from a suitable seed in the manner of any model described in this paper. D. Bell (cf. [Cal]) recently worked out one instance, a *unit Life cell* which lets Conway's rule simulate its own universe. As another illustration of universality, since any computer algorithm can be simulated, theoretically it should be possible to design a Life seed which grows with asymptotic isotropy.

Lest the reader conclude that anything is possible, so there is nothing to know, we hasten to point out two essential limitations of the simulation approach. First, it gives no information about how Life evolves starting from the preponderance of initial configurations, or from prescribed simple seeds. Second, even if the goal is to design prescribed dynamics – a finite  $A$  with period 17, say, or the delay-line memory architecture of the 1949 EDSAC computer – general theory is worthless for a manageable construction. Thus, a small group of dedicated researchers continues to do remarkable work on the *synthetic* understanding of Conway's rule, assembling a huge menagerie of known *objects*, and interactions between them which can be controlled despite Life's complexity. Paul Callahan's wonderful *Patterns, Programs and Links* web site [Cal] features annotated animations of more than a hundred key constructs. Another even more extensive web site maintained by Mark Niemiec [Nie] includes contact

information for most of the Life cadre mentioned in this review. Before proceeding to our discussion of persistent growth, let us mention a recent crowning achievement. Based on ten years of active experimentation by David Buckingham with B-heptomino interactions, there is now a general recipe for constructing a finite Life seed of *any* period greater than 57. At present, only fourteen periods are not yet known to arise within elementary objects:

19, 23, 27, 31, 33, 34, 37, 38, 39, 41, 43, 49, 51, and 53.

(Of these, the values 33, 34, 38, 39, and 51 can be achieved by non-interacting pairs of known objects with the required prime periods.)

### *Breeders and Spacefillers*

A glider gun generates persistent growth, albeit in a single direction, since it emits a steady stream of gliders which advance at constant rate. The first example of a Life seed with two-dimensional asymptotic shape was Gosper's 4060-cell *breeder* from the early 1970s. Nowadays the term is used to describe any pattern with a population that grows quadratically by creating a stream of objects, each of which creates another stream. Fig. 18 shows the smallest known breeder at present, due to Hickerson. In this variant, a “puffer” travels to the right at speed  $\frac{1}{2}$ , leaving a steady trail of guns behind, each of

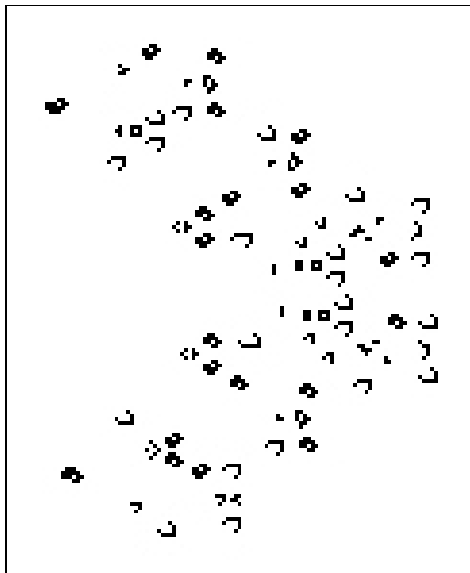


**Fig. 18.** Hickerson's 603 cell Breeder

which emits gliders traveling in the NE direction. The asymptotic effect is a triangular shape composed completely of gliders, occupying one out of every 45 cells in a regular array:

$$t^{-1}A_t \rightarrow \frac{1}{45}1_{\Delta}(x) dx, \quad \text{where } \Delta = \{0 < x_2 < x_1 < \frac{1}{2} - x_2\},$$

in the sense of (3.3). A more elaborate and very recent puffer/glider construction by Gosper yields a seed  $A_0$  from which Life evolves so that every site of  $\mathbb{Z}^2$  is occupied infinitely often by “waves of gliders going back and forth across a widening river” (a design proposal of Allan Wechsler), but such that the occupation times of each  $x$  form an aperiodic sequence.

One of the most remarkable Life constructions of the 1990s is *Max*, the *spacefiller*. First, the reader should understand that a *still life* is any configuration which is a fixed point for Conway's rule. For instance, a  $2 \times 2$  box is a still life. So is the density  $\frac{4}{9}$  periodic tiling of the lattice by such boxes separated by empty “frames” with width one. A spacefiller, then, is a seed  $A_0$  such that its limit  $A_\infty$  exists, and is a still life with positive density in  $\mathbb{Z}^2$ . The 187-cell seed *Max* at the upper left of Fig. 19

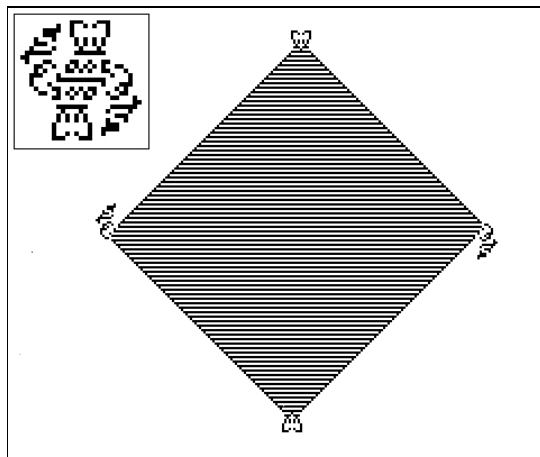


Fig. 19. Stripes generated by *Max*, a 187-cell Life spacefiller

generates a density  $\frac{1}{2}$  still life by spreading, as shown, in a diamond of alternating occupied and vacant horizontal stripes. The delicate “stretchers” at the corners advance at rate  $\frac{1}{2}$ , so


$$t^{-1}A_t \rightarrow \frac{1}{2}1_{\mathcal{D}_{\frac{1}{2}}}(x) \, dx, \quad \text{where } \mathcal{D}_{\frac{1}{2}} = \{\|x\|_1 \leq \frac{1}{2}\},$$


again in the sense of (3.3). *Max* has been dieting recently. The design shown here, currently the smallest known spacefiller, incorporates the combined efforts of H. Holzward, D. Bell, A. Hensel and T. Coe. *Max* is optimal in two additional respects. First, by comparison with Threshold 3 Growth, no Life configuration can advance on an empty background in the horizontal or vertical direction at speed greater than  $\frac{1}{2}$ . Second, N. Elkies has shown that  $\frac{1}{2}$  is the maximum possible density for a still life. In fact, he proves the following beautiful combinatorial generalization:

**Theorem 4 [Elk].** If every site  $x$  of configuration  $A \subset \mathbb{Z}^2$  has at most 3 range 1 box neighbors belonging to  $A$ , then  $\limsup_{n \rightarrow \infty} |A \cap B_n| / |B_n| \leq \frac{1}{2}$ .

In the same paper, Elkies obtains analogous sharp upper bounds if 3 in his theorem is replaced by any other possible value except 4 or 5, also solves the corresponding range 1 diamond problem completely, and discusses generalizations to higher dimensions and other graphs.

### *Nucleation Issues*

Nothing in our discussion of Conway's rule so far addresses the issue of whether “typical” seeds grow persistently. Most of the smallest configurations either die out or rapidly stabilize as a still life or oscillator, perhaps after emitting a few gliders. Early on, Life experimentalists coined the somewhat ill-defined notion of a *methuselah* – a small seed, of less than a dozen occupied cells say, which does not stabilize in a recursive pattern for a rather long time, say until at least  $t = 969$ . Perhaps the first example encountered was the *r*-pentomino , which stabilizes in generation 1103 after producing 6 gliders.

What, then, is the size of the smallest seed which generates persistent growth? This question is still open, although it may not remain so for long. By an exhaustive computer search, Nick Gotts and Paul Callahan have checked that no initial configuration of 8 or fewer cells grows persistently. Within the past few months Callahan has also discovered a 10 cell seed that does grow. His method was to test large collections of possible interactions between two minimal methuselaha with total population 10. One successful combination arises within a box 35 sites wide and 18 sites high: place an *r*-pentomino (oriented as above) in the upper left corner, and its 5-cell grandparent  in the lower right. After about 2000 iterations the evolution stabilizes, with a steady stream of gliders traveling SW. For now, there remains the possibility of persistent growth from 9 initially occupied sites, although Callahan feels he has ruled out “the most likely candidates.”

As we have seen throughout this paper, even for “supercritical” models one only expects persistent growth to be the norm once the initial seed is sufficiently large. Thus it is natural to pose

**Problem 20.** Do most finite Life seeds have infinite population growth? More precisely, if  $\varphi(n)$  denotes the number of configurations  $A \subset B_n$  such that  $|A_t| \rightarrow \infty$ , does  $\varphi(n)/2^{|B_n|} \rightarrow 1$  as  $n \rightarrow \infty$ ?

Dean Hickerson argues that the answer is undoubtedly “yes,” since a random huge pattern will include a speed  $\frac{1}{2}$  puffer moving outward somewhere along its boundary, output from which will cause the total population to grow. But this assertion is probably quite difficult to prove since some rare structure might conceivably chase along the puffer's trail, delete its output, and ultimately destabilize the puffer itself, in the manner of an LwoD shoot overrunning its ladder.

Finally, a most vexing issue is the classification of Conway's rule as “subcritical, critical, or supercritical.” This trichotomy is even hard to formulate for general CA dynamics, but in the spirit of Section 2, supercritical growth should spread over the whole lattice starting from almost any suitably large finite seed, subcritical growth should be unable to fill in large holes from typical exterior configurations, and the remaining alternative might well be deemed critical. Since the great preponderance of small Life seeds either die or stop growing within a few thousand updates, since there are apparently no known examples of persistent chaotic growth, and since Life on a large torus started from random initial conditions (e.g., the default screen saver of SUN Sparcstations for many years) eventually relaxes to a periodic state, it is natural to surmise that Life should be subcritical. On the other hand, attempts have been made to evaluate growth properties of Life by measuring its ability to propagate finite perturbations of a disordered equilibrium. Two contradictory conclusions have emerged: in [BCC] it was claimed to have a power law tail, and hence that Life enjoys *self-organized criticality*, whereas [BB] used larger, more extensive simulations on a CAM to conclude that effects die off exponentially quickly, albeit with a small exponential rate. What seems clear is that the Game of Life is remarkably close to critical, by any reasonable definition. In this vein, K. Evans [Eva] has studied higher-range generalizations of Conway's rule known as *Larger than Life*, finding a whole parameterized family of CA rules which are close to critical and support various glider-like bugs, breeders, replicators etc. To end on a paranoid note, Problem 19 raises the specter of some exotic, exceedingly rare architecture with the ability to outcompete any surrounding environment and spread supercritically over any environment, in a manner reminiscent of the stable periodic objects of [FGG1]. Life aficionados have never come close to encountering such a creature, but one might be lurking in another galaxy.

## 7. Remarks on Random Growth

Chance enters into growth dynamics in two natural ways: either by *random seeding*, i.e., by starting from a random configuration while keeping the update rule deterministic, or by a *random perturbation* of the update rule. In either case, there is a bewildering variety of ways to make the random assignments, so we will confine our discussion to the simplest choices. For concreteness, we also restrict the discussion to range 1 box solidification rules.

In the case of random seeding, we will assume that the initially occupied set  $A_0$  is obtained simply by adjoining every site independently with probability  $p$ . Such initializations are convenient since they are relatively easy to compute with, and convenient for simulation, while typically capturing the essential ergodic behavior of many other translation invariant initial states. Since we are dealing with solidification rules, the random set  $A_\infty = \{x : \xi_\infty(x) = 1\}$  is well-defined, and  $P(\xi_\infty(0) = 1)$  measures the final density of occupied sites. The immediate question facing us is whether the dynamics are likely

to fill in most of the lattice under these conditions. The first of the following two problems is not difficult to solve (see [GG2]), whereas the second is largely open.

**Problem 21.** Consider Threshold Growth with threshold  $\theta$  and seeding density  $p$ . Prove that for any  $p > 0$ , almost surely,  $A_\infty = \mathbb{Z}^2$  iff  $\theta \leq 4$ . Also, for the solidification rule which has  $\beta(i) = 1$  iff  $i = 1$  or  $i \geq 5$ , show that for any  $p \in (0, 1)$ ,  $P(\xi_\infty(0) = 1) \in (0, 1)$ .

**Problem 22.** For Exactly  $\theta$  Growth, when is  $\liminf_{p \rightarrow 0} P(\xi_\infty(0) = 1) > 0$ ? Simulations seem to suggest that this is the case for  $\theta \leq 3$ . Does the limit of final densities as  $p \rightarrow 0$  exist, and is it equal to  $\frac{4}{9}$  for Exactly 1 Growth?

The situation when seeding is sparse, i.e., for  $p$  small, is of particular interest, as it emulates crystal growth caused by rare impurities. In such circumstances the rate at which the dynamics fill space is of basic importance, and the natural statistic to measure this rate is  $T$ , the first time the origin is occupied. Simulations make it clear that, in the process of covering the lattice, the system evolves through three stages: (i) *nucleation* of occupied areas which are able to grow by themselves, (ii) *growth* in a slightly polluted environment, and (iii) *interaction* between large growing droplets. Understanding these aspects is crucial for estimating the size of  $T$ . For example, the following theorem holds.

**Theorem 5.** Let  $\xi_t$  be Threshold Growth with threshold  $\theta$  and seeding density  $p$ . In supercritical cases, i.e., for  $\theta \leq 3$ ,  $Tp^\theta$  converges in distribution to a nontrivial random variable as  $p \rightarrow 0$ . In the critical case  $\theta = 4$ , there exist two constants  $0 < c_1 < c_2 < \infty$  such that  $P(p \ln T \in [c_1, c_2]) \rightarrow 1$  as  $p \rightarrow 0$ .

Roughly, then,  $T$  is of order  $p^{-\theta}$  for supercritical dynamics, and of exponential size in  $\frac{1}{p}$  for critical dynamics. In the latter case, the origin is likely to wait a prolonged time of *metastability* before it gets occupied. The metastable period, which is exponentially large in a power of  $\frac{1}{p}$  is a signature property of critical thresholds for neighborhoods which are invariant under 90-degree rotation. References [AL], [GG2], [GG5], [Mou] and [Sch] include further discussion of metastability effects in various models.

The more precise statement of Theorem 5 in the supercritical case is possible because the nucleation positions can be scaled by  $p^\theta$  to yield a Poisson point location. (For general  $\mathcal{N}_\rho$ , the correct scaling is  $p^\gamma$ .) On this scale, the growth and interaction phases involve polygonal shapes which evolve in a computable way in continuous space and time. We refer the reader to [GG2] for a complete proof, but include a problem here which should illuminate at least the nucleation ingredient of the argument.

**Problem 23.** For a general solidification rule, define  $\gamma$  as the size of the smallest initial set  $A_0$  which generates persistent growth. Assuming  $\gamma < \infty$ , label  $x \in \mathbb{Z}^2$  a *nucleus* if there exists a set  $A_0$  of  $\gamma$  initially occupied sites such that (i)  $A_0$  generates persistent growth, and (ii)  $x$  is the leftmost of the lowest points of  $A_0$ . Compute  $\lim_{p \rightarrow 0} p^{-\gamma} P(x \text{ is a nucleus})$ . Then do the same if (i) is replaced by (i')

$$T^\infty(A_0) = \mathbb{Z}^2.$$

The suggested computations (more suitable for a computer than a human) should provide some insight about nucleation properties of range 1 solidification rules. For supercritical Threshold Growth, the common value of the above two limits determines the intensity (number of points per unit area) of the Poisson point location described above.

To illustrate how shape theory applies to related systems, we briefly mention the Multitype Threshold Voter Model. In this CA one starts with a uniform product measure over  $\kappa$  colors on the lattice and, at each update, site  $x$  changes to color  $k$  iff  $k$  is the *unique* color with at least  $\theta$  representatives in  $x + \mathcal{N}$ . As  $\kappa$  becomes very large, widely separated regions of single color start expanding, until they eventually induce a division of available space. If the space is scaled by  $\kappa^{1-\theta}$  (note that  $\theta$  must be at least 2 for anything to happen), then this division approaches a *Poisson-Voronoi* tessellation of  $\mathbb{R}^2$ . This is the object constructed by assigning every point in a Poisson point location  $\mathcal{P}$  its own color, and then painting every other point in  $\mathbb{R}^2$  the same color as the closest color in  $\mathcal{P}$ . The limit shape  $L$  of the corresponding Threshold Growth model determines the norm in which distance is measured.

The rest of this section is devoted to randomly perturbed dynamics. Assuming that growth is generated by a deterministic monotone transformation  $\mathcal{T}$ , and that  $p \in [0, 1]$  is a fixed *update probability*, we confine our discussion to the following simple randomized algorithm:

(a) Let  $X_{x,t}$ ,  $x \in \mathbb{Z}^2$ ,  $t = 0, 1, 2, \dots$ , be an independent family of Bernoulli ( $p$ ) random variables, i.e.,

$$P(X_{x,t} = 1) \equiv p \equiv 1 - P(X_{x,t} = 0).$$

(b) Start from some (deterministic or random) set  $A_0$ , independent of  $X_{x,t}$ . Given  $A_t$ , the random set  $A_{t+1}$  is determined as

$$A_t \cup \{x \in \mathcal{T}(A_t) : X_{x,t} = 1\}..$$

Such a process is therefore a Markov chain on subsets of  $\mathbb{Z}^2$ . Dynamics in this vein have been widely studied for more than twenty years. One of the first and most famous examples, in which  $\mathcal{T}$  is Threshold Growth with range 1 diamond neighborhood and  $\theta = 1$ , is called *Richardson's model* [**Ric**]. Related threshold 1 systems with random births and random deaths (often run in continuous time) are Eden's crystal growth [**Ede**], voter models [**Durr**], [**Toom**] and the contact process [**DG1**]. Many papers have



been devoted to shape theory for such local rules. The only known approach is subadditivity, so existence of shapes and rates of convergence are within reach of rigorous mathematics, but explicit computations are not. By contrast, it *is* possible to explicitly compute shapes when they result from aggregate behavior of random walks. Two such examples are: branching random walks, which are tractable by projection onto lines, in terms of (anisotropic) large deviation rates [Big]; and Internal DLA, which inherits *circular* shape from isotropy of the continuum space-time limit [LBG], [GQ].

A common feature of the rules described above is that the limiting shape is a convex set, hence about as regular as Euclidean sets can be. At the opposite extreme are models like DLA [WS], which apparently approach some random fractal. Although a lot is known about such dynamics from the physics literature [BS], rigorous results are few and far between.

To reiterate, subadditivity is apparently the only general tool for proving convergence of a random sequence of sets, given by (a) - (b) above, to an asymptotic shape. The two alternative approaches described in previous sections – explicit recursion, or identification of half-space velocities – seem hopeless. Moreover, even the subadditivity arguments which have been applied to random dynamics rely on a self-evident property of Threshold 1 Growth: the process can be *restarted* from any occupied cell. To illustrate how subadditivity works in the presence of randomness, *and* how to handle thresholds  $\theta > 1$ , we will now outline the proof of a shape theorem for the randomized version of our Basic Example.

**Theorem 6.** Consider Random Threshold Growth on the range 1 box neighborhood, with  $\theta = 3$  and update probability  $p > 0$ . Then there exists a convex compact neighborhood of the origin,  $0 \in L \subset \mathbb{R}^2$ , such that

$$t^{-1}A_t \xrightarrow{H} L \quad \text{for every finite } A_0 \text{ such that } \mathcal{T}^\infty(A_0) = \mathbb{Z}^2.$$

**Proof.** Let  $\tau$  denote a geometric random variable with parameter  $p$  (i.e.,  $P(\tau = k) = p(1 - p)^{k-1}$ ;  $k \geq 1$ ). Moreover, assume that  $A_0 = B_\infty(0, 1)$ ; this entail no loss of generality since a seed which generates the plane under  $\mathcal{T}$  will cover this square in a finite time under the random dynamics. Now define

$$\begin{aligned} T(x) &= \inf \{t : x \in A_t\}, \\ T'(x) &= \inf \{t : x + B_1 \subset A_t\}, \\ T'(x, y) &= \inf \{t : y + B_1 \subset A_{t+T'(x)}(x + B_1, T'(x))\} \end{aligned}$$

Here  $A_{t+u}(B, u)$  is notation for the state of the process at time  $t + u$  if it is restarted from  $B$  at time  $u$ . Write  $A'_t = \{x : x + B_1 \subset A_t\}$ . Our first step is to prove that  $A_t$  does not extend too far beyond  $A'_t$ .

The Lemma from Section 2 implies that  $T'(x) - T(x)$  is bounded above by the sum of 25 independent copies of  $\tau$ , since in the worst case sites inside  $B_\infty(x, 2)$  are added one by one. (The number 25 can be reduced somewhat.) The following crude bound therefore holds for any  $u \geq 0$ ,

$$(7.1) \quad P(T'(x) - T(x) \geq u) \leq 25 \cdot P(\tau \geq u/25) \leq 25 e^{-pu/25}.$$

Of course  $A_t \subset \mathcal{T}^t(A_0)$ , so  $A_t$  includes at most  $(2t+3)^2$  sites. Therefore, for large  $t$ ,

$$P(T'(x) - T(x) > \frac{100}{p} \log t \text{ for at least one } x \in A_t) \leq (2t+3)^3 \cdot 25 \cdot e^{-4 \log t} \leq 200 \cdot t^{-2},$$

and hence, by the Borel-Cantelli lemma, there exists a random  $T_0$  such that  $T'(x) - T(x) \leq \frac{100}{p} \log t$  for every  $x \in A_t$  as soon as  $t \geq T_0$ . It follows that

$$(7.2) \quad A'_t \subset A_t \subset A'_{t + \frac{100}{p} \log t} \quad \text{for } t \geq T_0.$$

The last step uses subadditivity to show that  $A'_t$  has a limiting shape. By monotonicity,  $T'(y) \leq T'(x) + T'(x, y)$ . In addition, the last two summands are independent, and  $T'(x, y)$  has the same distributions as  $T'(y - x)$ . Moreover, if  $e_1 = (1, 0)$ , then the argument leading to (7.1) also shows that, for every  $u \geq 0$ ,  $P(T'(e_1) > u) \leq 25 \cdot \exp\{-pu/25\}$ . In particular,  $E[T'(x)] < \infty$  for every  $x$ . Moreover, if  $\delta = p/1000$ , and  $T'_1, T'_2, \dots$  are independent copies of  $T'(e_1)$ , then

$$(7.3) \quad \begin{aligned} P(B_{\delta t} \not\subset A'_t) &\leq (2\delta t + 1)^2 P\left(\sum_{i=1}^{2\delta t} T'_i > t\right) \\ &= (2\delta t + 1)^2 P\left(\exp\left\{\frac{p}{50} \sum_{i=1}^{2\delta t} T'_i - \frac{p}{50} t\right\} \geq 1\right) \\ &\leq (2\delta t + 1)^2 \exp\left\{-\frac{p}{50} t\right\} \cdot E\left[\exp\left\{\frac{p}{50} T'(e_1)\right\}\right]^{2\delta t} \\ &\leq (2\delta t + 1)^2 \exp\left\{-\frac{p}{50} t\right\} \cdot (50)^{2\delta t} \\ &\leq \exp\left\{-\frac{p t}{100}\right\}, \end{aligned}$$

so that, with probability one,  $A'_t$  eventually includes  $B_{\delta t}$ .

From this point on, the argument proceeds along standard lines (as in Chapter 1 [Durr], and [CD]). First one extends  $T'$  to  $x \in \mathbb{R}^2$  by:  $T'(x) = \inf\{t : x \in A'_t + I\}$ , where  $I$  is the Euclidean square  $[-\frac{1}{2}, \frac{1}{2}]^2$ . Then the Subadditive Ergodic Theorem (cf. [Dur]) is applied to conclude that, for every  $x \in \mathbb{R}^2$ ,

$$(7.4) \quad n^{-1} T'(nx) \rightarrow v(x) \quad \text{with probability one, as } n \rightarrow \infty,$$

where  $v(x)$  is the deterministic limiting velocity in the direction of  $x$ . Function  $v$  is a norm on  $\mathbb{R}^2$ .

Convergence (7.4) for all  $x$  in a suitable finite set, together with lower bound (7.3), implies that the unit ball  $L = \{x : v(x) \leq 1\}$  is the limiting shape:  $t^{-1}A'_t \xrightarrow{H} L$ . This fact, in combination with (7.2), completes the proof.  $\square$

An essential ingredient in the above proof is the Lemma from Section 2. It turns out that a version of that deterministic result holds in considerable generality [BG], but the complete answer is known only for Threshold Growth on range  $\rho$  box neighborhoods. In that case, an occupied point sees a large set within  $\ell^\infty$  distance  $R = 1000 \rho^3 (1 + \log \rho)$ . More precisely, for every  $x \in A_t$  which is not within  $\ell^\infty$  distance  $R$  of  $A_0$ , there is a set  $G \subset A_t \cap (x + B_R)$  such that  $T^\infty(G) = \mathbb{Z}^2$ . Given this property, it is not hard to make appropriate modifications in the above proof and conclude that Theorem 6 extends to general box neighborhoods and arbitrary thresholds.

As already mentioned, analytic identification of the limiting shape seems impossible for nearly all random growth models. However, partial information is available in a few instances. The best-known example is Richardson's model: if  $p > p_c$ , the critical probability for oriented site percolation, then the shape  $L$  has flat edges [DL]. (It is believed that  $p_c \approx .706$ , but the best available rigorous upper bound at present is  $p_c < .819$ .) It is also sometimes possible to approximate  $L$  in a nearly deterministic model. For example, as  $p \rightarrow 1$ , the shape of Richardson's model converges to the unit diamond. A more difficult example is the solidification rule in which a site with exactly one of its four nearest neighbors becomes occupied at each update with probability  $p$ , while two or more occupied neighbors make it occupied for sure. In this case, it is not hard to show that the asymptotic shape  $L_p$  exists, but more to the point is that  $p^{-\frac{1}{2}}L_p$  converges to a square (of unknown side) as  $p \rightarrow 0$  [KeSc], [Gra2].

Since techniques for explicit computation of limit shapes for random dynamics are lacking, we resort to Monte Carlo simulation. Running the dynamics from finite sets has some serious drawbacks: the convergence is slow, while strict convexity and differentiability properties are very difficult to detect. A more expeditious approach assumes validity of the polar formula  $L_p = K_{1/w_p}^*$ , and proceeds to estimate the half-space speeds  $w_p$ . Efficient estimation of these speeds is possible since one can reduce random fluctuations by averaging, exploiting the fact that half-spaces are translation invariant in one direction. While this approach yields interesting results, as we shall see below, it unfortunately has no theoretical foundation at present. The models for which half-space velocities can be proved to exist are limited to those which admit either a first-passage [Kes2] or last-passage [Gra2] representation. Beyond such examples, even the special case stated in our next problem remains unresolved at the rigorous level. However this has not stopped physicists from developing voluminous and sophisticated theory on the regularity of interface motion (see, e.g., [KrSp], [BS]).

**Problem 24.** Consider, again, Random Threshold Growth with  $\theta = 3$ . Let  $A_0$  consist of sites on or below the  $x$ -axis, and let  $V_t \subset \mathbb{Z}$  comprise the second coordinates of the intersection of  $A_t$  with the  $y$ -axis. Show that

$$w_p(e_2) = \lim_{t \rightarrow \infty} t^{-1} \max V_t = \lim_{t \rightarrow \infty} t^{-1} \min (\mathbb{Z}^2 - V_t)$$

exists with probability one.

Overlooking the current lack of a proof that half-space speeds exist, we now present some intriguing computer simulations which estimate  $K_{1/w_p}$  and  $L_p$  for Random Threshold Growth with  $\theta=3$  and various values of  $p$ . Figure 20 shows the results for  $p = 1, \frac{9}{10}, \dots, \frac{4}{10}$ . Of course the sets  $K$  on the left increase as  $p$  decreases, whereas the shapes  $L$  on the right decrease.

- (a) If  $p$  is very close to 1, then the convex hull of  $K_p$  is the same as the convex hull of  $K_1$ . In this case  $L_p = L_1$ , so the shape is an explicitly computable polygon.
- (b) As  $p$  decreases, eventually the boundary of  $K_p$  no longer intersects the boundary of  $K_1$ . In this case the boundary of  $K_p$  is smooth, but if  $p$  is not too small, then  $K_p$  is still non-convex. Hence  $L_p$  has a non-differentiable boundary (i.e., “corners”), but no flat edges.

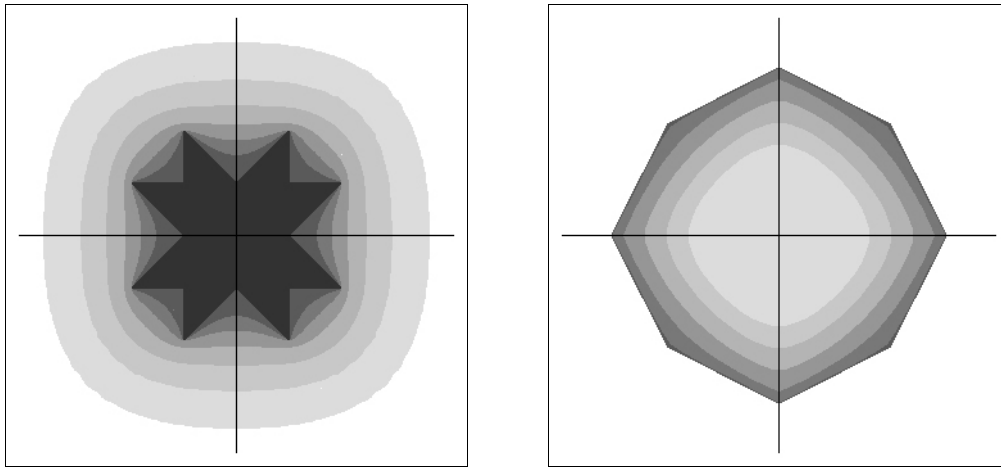


**Fig. 20.**  $K_{1/w_p}$  (left) and  $L_p$  (right) for  $p = 1, .9, \dots, .4$

- (c) Further decreased values of  $p$  seem to produce a smooth strictly convex  $K_p$ . While the mechanism which causes the onset of this regime remains mysterious, the resulting shapes are apparently smooth and strictly convex.

Whether or not there is a phase between (a) and (b) in which  $L$  is not a polygon but still has both corners and flat edges seems too subtle to predict from our simulations, but that fourth scenario seems likely for at least some choices of neighborhood and threshold. We remark that smoothness of the

limiting shapes is important in understanding boundary fluctuations of random growth [NP]. More details on these issues, including rigorous proofs of some of the observations described above, will appear in a forthcoming research paper [BGG].

One feature of supercritical Threshold Growth models is that small random perturbations do not change their long-term behavior appreciably. For instance, in the example just discussed,  $L_p \rightarrow L_1$  as  $p \rightarrow 1$  (with equality in a small neighborhood of  $p = 1$ ). By contrast, any random perturbation may destroy the delicate growth pattern of a non-monotone rule. The reader can either try to work out the solution to our next problem (which is rather difficult; see [BN] for the appropriate technology), or else trust Fig. 21, which shows a realization of the Random Exactly 1 CA with  $p = .95$ , after 55 updates, started from a single occupied cell. Note how the fractal pattern of Figure 6 is completely destroyed.

**Problem 25.** Consider the Random Exactly 1 CA with update probability  $p$ . Show that, for every  $\epsilon > 0$ , there exists a  $p_0$  such that, for every update probability  $p \in (p_0, 1)$ , a large enough time  $T$  exists with probability one, so that for any  $t \geq T$ ,

$$\mathcal{B}_{1-\epsilon} \subset t^{-1}A_t + \mathcal{B}_\epsilon$$

(where both boxes above are Euclidean).

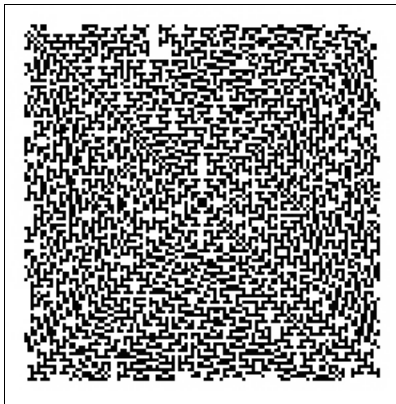


**Fig. 21.** Random Exactly 1 growth from a singleton,  $p = .95$

In short, the limiting shape, if it exists, is close to the unit square for  $p$  close to 1. The statement in Problem 22 is convoluted since  $L$  is not known to exist. Indeed, except for trivial cases, no techniques are currently available to prove existence of a limiting shape for any random non-monotone model. The relatively simple Random Exactly 1 rule might offer the best prospects for development of such techniques. We therefore make it the subject of our last open problem.

**Problem 26.** Show that the Random Exactly 1 rule with update probability  $p$ , started from any (non-empty) finite seed  $A_0$ , has a unique asymptotic shape  $L$ .

## 8. Appendix: CA Computation and Visualization Resources

The Primordial Soup Kitchen [Gri2]:

<http://psoup.math.wisc.edu/kitchen.html>

is an extensive Web site devoted to cellular automata. Included are an annotated archive of colorful images illustrating the theory and application of CA rules, electronic versions of several of our research papers, and the *WinCA* [FG] software which was used to perform most of the experiments discussed here, as well as links to other sites on the Internet which deal with complex spatially-distributed systems. A page at the same site,

<http://psoup.math.wisc.edu/java/growth.html>

has been produced specifically to supplement this article. There the reader will find a Java applet which runs small-scale, device-independent animations of many of the growth models we have discussed, together with ready-made *WinCA* data files for larger and much faster versions of the same experiments, and up-to-date Web links to additional resources concerning CA shapes.

**Acknowledgments.** We are grateful to Tom Bohman, Paul Callahan, Bruce Christenson, Kellie Evans, Bob Fisch, Cris Moore, Norm Margolus and Stephen Wolfram for their contributions. Special thanks to Dean Hickerson for permission to reproduce several of his remarkable experiments and results.

## REFERENCES

- [AL] M. Aizenman, J. Lebowitz, *Metastability effects in bootstrap percolation*, J. Phys. A: Math. Gen. **21** (1988), 3801-3813.
- [Ban] E. R. Banks, *Universality in cellular automata*, in Proc. 11th IEEE Symposium on Foundations of Computer Science (FOCS) (1970), 194-215.
- [BB] C. Bennett, M. Bourzutschky, “*Life*” not critical?, Nature **350** (1991), 468.
- [BCC] P. Bak, K. Chen, M. Creutz, *Self-organized criticality in the “Game of Life,”* Nature **342** (1989), 780.
- [BCG] E. Berlekamp, J. Conway, R. Guy, *Winning Ways for Your Mathematical Plays*, vol. 2, chapter 25, Academic Press, New York, 1982.
- [Big] J. Biggins, *The asymptotic shape of the branching random walk*, Advances in Appl. Probability **10** (1978), no. 1, 62-84.
- [Boh] T. Bohman, *Discrete Threshold Growth dynamics are omnivorous for box neighborhoods*, Trans. Amer. Math. Soc. (1997), to appear.
- [BG] T. Bohman, J. Gravner, *Random threshold growth models*, (1997), submitted.
- [BGG] T. Bohman, J. Gravner, D. Griffeath, *Asymptotic shapes for random threshold growth models*, (1997), in preparation.

- [BH] S. Broadbent, J. Hammersley, *Percolation processes. I. Crystals and mazes*, Proc. Cambridge Philos. Soc. **53** (1957), 629-641.
- [BN] M. Bramson, C. Neuhauser, *Survival of one-dimensional cellular automata under random perturbations*, Ann. Prob. **22** (1994), 244-263.
- [BS] A.-L. Barabasi, H. Stanley, *Fractal concepts in surface growth*, Cambridge University Press, 1995.
- [Cal] P. Callahan, *Patterns, Programs, and Links for Conway's Game of Life*, <http://www.cs.jhu.edu/~callahan/lifepage.html>.
- [CD] J. T. Cox, R. Durrett, *Some limit theorems for percolation processes with necessary and sufficient conditions*. Ann. Prob. **9** (1981), 583-603.
- [Dura] B. Durand, *Inversion of 2D cellular automata: some complexity results*, Theoretical Computer Science **134** (1994), 387-401.
- [Durr] R. Durrett, *Lecture Notes on Particle Systems and Percolation*, Wadsworth & Brooks/Cole, 1988.
- [DG1] R. Durrett, D. Griffeath, *Contact processes in several dimensions*, Z. Wahrscheinlichkeitstheorie verw. Gebiete **59** (1982), 535-552.
- [DG2] R. Durrett, D. Griffeath, *Asymptotic behavior of excitable cellular automata*, J. Experimental Math. **2** (1993), 183-208.
- [DKS] R. Dobrushin, R. Kotecky, S. Shlosman, *Wulff Construction, A Global Shape from Local Interaction*, American Mathematical Society, 1992.
- [DLi] R. Durrett, T. Liggett, *The shape of the limit set in Richardson's growth model*, Ann. Prob. **9** (1981), 186-193.
- [DS] R. Durrett, J. Steif, *Fixation results for the threshold voter models*, Ann. Prob. **21** (1993), 232-247.
- [EE-K] G. Ermentrout, L. Edelstein-Keshet, *Cellular automata approaches to biological modeling*. *J. Theor. Biol.* **160** (1993), 97-133.
- [Ede] M. Eden, p.359 in Symp. on Information Theory in Biology, ed. H. Yockey, Pergamon Press, New York, 1958.
- [Elk] N. Elkies, *The still-Life density problem and its generalizations*, preprint, 1997.
- [Eva] K. Evans, *Larger than Life: it's so nonlinear*, Ph.D. dissertation, Univ. of Wisconsin, 1996.
- [FG] R. Fisch, D. Griffeath, *WinCA: a cellular automaton modeling environment*, Windows 3.x/95 software, version 1.0, 1996. Available from [Gri2].
- [FGG1] R. Fisch, J. Gravner, D. Griffeath, *Threshold-range scaling of excitable cellular automata*, Statistics and Computing **1** (1991), 23-39.
- [FGG2] R. Fisch, J. Gravner, D. Griffeath, *Metastability in the Greenberg-Hastings model*, Ann. Appl. Prob. **3** (1993), 935-967.
- [FHP] U. Frisch, B. Hasslacher, Y. Pomeau, *Lattice-Gas Automata for the Navier-Stokes Equation*, Phys. Rev. Lett. **56** (1986), 1505-1508.
- [Gar1] M. Gardner, *Mathematical Games - The Fantastic Combinations of John Conway's New Solitaire Game, Life*, Scientific American, October 1970, 120-123. Subsequent articles about Conway's Life appeared in the *Mathematical Games / Computer Recreations* column of Scientific American, in the issues of Nov 70, Jan 71, Feb 71, Mar 71, Apr 71, Nov 71, Jan 72, Dec 75, Mar 84, May 85, Feb 87, Aug 88, Aug 89, Sep 89, and Jan 90.

- [Gar2] M. Gardner, *Wheels, Life and Other Amusements*, Freeman, 1983.
- [Garz] M. Garzon, *Models of Massive Parallelism: Analysis of Cellular Automata and Neural Networks*, Springer-Verlag, 1995.
- [GHH] J. Greenberg, B. Hassard, S. Hastings, *Pattern formation and periodic structures in systems modeled by reaction-diffusion equations*, Bull. AMS **84** (1978), 1296-1327.
- [Gra1] J. Gravner, *The boundary of iterates in Euclidean growth models*, T.A.M.S. (1996), 4549-4559.
- [Gra2] J. Gravner, *Recurrent ring dynamics in two-dimensional cellular automata*, (1996), submitted.
- [GG1] J. Gravner, D. Griffeath, *Threshold Growth dynamics*, T.A.M.S. (1993), 837-870.
- [GG2] J. Gravner, D. Griffeath, *First-passage times for discrete Threshold Growth dynamics*, Ann. Prob. (1996), 1752-1778.
- [GG3] J. Gravner, D. Griffeath, *Multitype Threshold Growth: convergence to Poisson-Voronoi tessellations*, Ann. Appl. Prob. **7** (1997), 615-647.
- [GG4] J. Gravner, D. Griffeath, *Nucleation parameters for discrete threshold growth dynamics*, Experimental Math. **6** (1997), 207-220.
- [GG5] J. Gravner, D. Griffeath, *Scaling limits for critical Threshold Growth* (1997), in preparation.
- [GHR] R. Greenlaw, H. Hoover, and W. Ruzzo, *Limits to Parallel Computation: P-Completeness Theory*, Oxford University Press, 1995.
- [GN] R. Gaylord, K. Nishidate, *Modeling Nature: Cellular Automata Simulations with Mathematics*, Springer-Verlag, 1996.
- [GQ] J. Gravner, J. Quastel, *Internal DLA and the Stefan problem* (1998), in preparation.
- [Gri1] D. Griffeath, *Self-organization of random cellular automata: four snapshots*, In *Probability and Phase Transitions*, ed. G. Grimmett, Kluwer, 1994.
- [Gri2] D. Griffeath, *Primordial Soup Kitchen*, <http://psoup.math.wisc.edu/kitchen.html>, World Wide Web.
- [GM] D. Griffeath, C. Moore, *Life without Death is P-complete* (1997), submitted.
- [Gut] H. Gutowitz, *Frequently asked questions about cellular automata*, <http://alife.santafe.edu/alife/topics/cas/ca-faq/ca-faq.html>, World Wide Web.
- [Har] J. Hartmanis, *On the Computing Paradigm and Computational Complexity*, MFCS'95, eds. J. Wiederman, P. Hajek, Springer LNCS No.969, 1995, pp. 82-92.
- [Hol] J. Holland, *Outline for a logical theory of adaptive systems and other articles*, In *Essays on Cellular Automata*, ed. Arthur W. Burks, University of Illinois Press, 1970.
- [Jen] E. Jen, *Exact solvability and quasiperiodicity of one-dimensional cellular automata*, Nonlinearity **4** (1991), 251-276.
- [JM] W. Johnson, R. Mehl, *Reaction kinetics in processes of nucleation and growth*, Trans. A.I.M.M.E. **135** (1939), 416-458.
- [Kar] J. Kari, *Reversibility of 2D cellular automata is undecidable*, Physica D **45** (1990), 379-385.
- [Kes1] H. Kesten, *First passage percolation and a higher-dimensional generalization*, in *Particle Systems, Random Media and Large Deviations* ed. R. Durrett, American Mathematical Society, 1984.



- [Kes2] H. Kesten, *On the speed of convergence in first-passage percolation*, Ann. Appl. Prob. **4** (1994), 76-107.
- [KeSc] H. Kesten, R. Schonmann, *On some growth models with a small parameter*, Probab. Th. Rel. Fields 101 (1995), 435-468.
- [KrSp] J. Krug, H. Spohn, *Kinetic roughening of growing surfaces*, in Solids far from Equilibrium, ed. C. Godreche, Cambridge University Press, 1882, 479-582.
- [Lan] C. Langton, *Studying Artificial Life with Cellular Automata*, Physica D **22** (1986), 120-149.
- [LDKB] A. Lawniczak, D. Dab, R. Kapral, and J.-P. Boon, *Reactive lattice gas automata*, Physica D **47** (1991), 132-158.
- [LBG] G. Lawler, M. Bramson, D. Griffeath, *Internal diffusion limited aggregation*, Ann. Prob. **14** (1992), 2117-2140.
- [Lig] T. Liggett, *Interacting Particle Systems*, Springer-Verlag, 1985.
- [Lin] D. Lind, *Applications of ergodic theory and sofic systems to cellular automata*, Physica 10 D (1984), 36-44.
- [LN] K. Lindgren and M. Nordahl, *Universal Computation in Simple One-Dimensional Cellular Automata*, Complex Systems **4** (1990), 299-318.
- [Marg] N. Margolus, *CAM-8: a virtual processor cellular automata machine*, MIT Laboratory for Computer Science (1995).
- [Mart] B. Martin, *A universal cellular automaton in quasi-linear time and its S-m-n form*, Theoretical Computer Science **123** (1994), 199-237.
- [Min] M. Minsky, *Computation: Finite and Infinite Machines*, Prentice Hall, 1972.
- [Mou] T. Mountford, *Critical lengths for semi-oriented bootstrap percolation*, Stochastic Process. Appl. **95** (1995), 185-205.
- [Nie] M. Niemiec, *Life Page*, <http://home.sprynet.com/interserv/mniemiec/lifepage.htm>.
- [NP] C. Newman, M. Piza, *Divergence of shape fluctuations in two dimensions*, Ann Prob. **23** (1995), 977-1005.
- [NM] M. Nowak and R. May, *Evolutionary games and spatial chaos*, Nature **359** (1992), 826-829.
- [Pac] N. Packard, *Cellular automaton models for dendritic crystal growth*, Institute for Advanced Study (1985).
- [Pap] C. Papadimitriou, *Computational Complexity*, Addison-Wesley, 1994.
- [PW] N. Packard, S. Wolfram, *Two-dimensional cellular automata*, J. Stat. Phys. **38** (1985), 901-946.
- [Ric] D. Richardson, *Random growth in a tessellation*, Proc. Camb. Phil. Soc. **74** (1973), 515-528.
- [San] L. Sander, *Fractal growth processes*, Nature **322** (1986), 789-793.
- [Sch] R. Schonmann, *On the behavior of some cellular automata related to bootstrap percolation.*, Ann. Prob. **20** (1992), 174-193.
- [TCH] J. Taylor, J. Cahn, C. Handwerker, *Geometric models of crystal growth* (Overview no. 98-1), Acta Met. **40** (1992), 1443-1474.
- [TM] T. Toffoli, N. Margolus, *Cellular Automata Machines – a new environment for modeling*, MIT Press, 1987.

- [Toom] A. Toom, *Cellular automata with errors: problems for students of probability*, in *Topics in Contemporary Probability and Its Applications*, edited by J. Laurie Snell, CRC Press, 1995.
- [Ula] S. Ulam, *Random Processes and Transformations*, Proc. (1950) Int. Congr. Mathem., **2** (1952), 264-275.
- [Vic] G. Vichniac, *Simulating physics with cellular automata*, Physica **10D** (1984) 96-115.
- [vK] H. von Koch, 1904.
- [vN] J. von Neumann, *Theory of Self-Reproducing Automata*, (ed. A Burks), Univ. of Illinois Press, 1966.
- [WR] N. Weiner, A. Rosenblueth, *The mathematical formulation of the problem of conduction of impulses in a network of connected excitable elements, specifically in cardiac muscle*, Arch. Inst. Cardiol. Mexico **16** (1946), 205-265.
- [WS] T. Witten, L. Sander, *Diffusion limited aggregation*, Phys. Rev. Lett. **47** (1981), 1400-1403.
- [Wil1] S. Willson, *On convergence of configurations*, Discrete Math. **23** (1978), no. 3, 279-300.
- [Wil2] S. Willson, *Cellular automata can generate fractals*, Discrete Appl. Math. **8** (1984), no. 1, 91-99.
- [Wol1] S. Wolfram, *Cellular Automata and Complexity*, Addison-Wesley, Menlo Park, CA, 1994.
- [Wol2] S. Wolfram, Private communication, 1995.

